Pathophysiological roles of aquaporin-4 in CNS disease

By

Didrik Søli Frydenlund

Dissertation for the degree of Philosophiae Doctor (PhD)

Center for Molecular Biology and Neuroscience

Faculty of Medicine

University of Oslo

2011

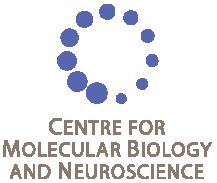

Series of dissertations submitted to the
Faculty of Medicine, University of Oslo
No. 1124

ISBN 978-82-8264-069-5

Cover: Inger Sandved Anfinsen.
Printed in Norway: AIT Oslo AS.

Produced in co-operation with Unipub.
The thesis is produced by Unipub merely in connection with the
thesis defence. Kindly direct all inquiries regarding the thesis to the copyright
holder or the unit which grants the doctorate.

TABLE OF CONTENTS

1. ACKNOWLEDGEMENTS

This thesis is the result of my work at the *Centre for Molecular Biology and Neuroscience* at the University of Oslo.
I would like to express my gratitude to all those who gave me the possibility to complete this thesis. First, I would like to thank my supervisors, Mahmood Amiry-Moghaddam and Tone Tønjum for their friendliness and optimistic approach to my projects. More specifically, Mahmood became my supervisor back in 2004 when I as a fresh medical student joined the group as a *Forskerlinje*-student. I thank him for his proactive attitude.
Tone Tønjum became my co-supervisor as I joined the *Meningitis project* at the start of 2009. Tone has been extremely optimistic on my behalf and has made substantial effort to keep the progress going and secure funds. Under her guidance, I have collaborated very closely with Tonje Davidsen and Cesilie Castellanos and spent endless hours at the animal facility. I thank them for a fruitful collaboration. Also, I must not forget to grant former group leader Ole Petter Ottersen, until he became the rector at the University of Oslo, he was my co-supervisor. I especially thank him for guiding me to write scientific papers.
I thank all the co-authors and my colleagues at the Laboratory for Molecular Neuroscience for providing an inspiring and competitive atmosphere. I would especially acknowledge:

- Torgeir Holen, whom his extensive knowledge has been an inspiring lab mate and given me valuable feed-back.

- Carina Knudsen for helping me with the illustration and figures for my papers and her always energetic and inspiring attitude.

- Tom Tallak Solbu who has willingly shared his extensive lab-skills teaching me how to do Western blot.

- Lisa Olsson for much needed help with the biochemical analysis.

- Bjørg Riber, Karen Marie Gujord and Jorunn Knutsen, for their positive and helpful attitude.

- Erlend Nagelhus for helping me to understand the art of postembedding immunocytochemistry and his willingness to discuss scientific issues with me.

- Finn-Mogens Haug, for spending endless hours with me deliberating image analysis issues.

- Johannes Helm, for his exceptional friendliness and for helping me out with technological emergencies at nights and weekends.

My salary was covered by a one year grant from the *Letten Foundation* and one year was covered by the CMBN; divided by 6 months from Tone Tønjum's group and 6 months from Mahmood Amiry-Moghaddam's group. Paper I and II were published while I was a follow at "Forskerlinjen": A MD PhD curriculum at the Faculty of Medicine.
I express my gratitude to my family and friends for patience and support.

2. ABBREVIATIONS

AQP - aquaporin

AVP – vasopressin

CAMK – calcium/calmodulin-dependent protein kinase

cAMP – cyclic adenosine monophosphate

cDNA – complementary deoxyribonucleic acid

CBF – cerebral blood flow

CNS – central nervous system

CSF – cerebrospinal fluid

DAPC – dystrophin-associated protein complex

DWI MRI – diffusion-weighted magnetic resonance imaging

ECS – extracellular space

FRIL – freeze-fracture immunogold labeling

GA – glutaraldehyde

HSA – human serum albumin

ICP – intracranial pressure

IMP – intramembrane particles

KO – knock-out

LOS – lipooligosaccharide

MAPK – mitogen-activated protein kinase

MC – meningococcus

MCA – middle cerebral artery

MCAO – middle cerebral artery occlusion

MMP – matrix metalloproteinase

NOS – nitric oxide synthase

NMO – neuromyelitis optica

OAP – orthogonal array of particles

PC – pneumococcus

PCR – polymerase chain reaction

PDZ – postsynaptic density 95, discs large, zonula occludens-1

PLC – phospholipase C

SNP – single nucleotide polymorphism

$V1_aR$ – vasopressin receptor type 1_a

WT – wild type

3. ERRATUM

Introduction

p. 38. Line 19 and 20. Deleted a feedback sentence from supervisor in Norwegian.

Manuscript III

p. 9. Added reference line 20, after word 7: [Gunnarson E. et al. Identification of a molecular target for glutamate regulation of astrocyte water permeability. Glia.2008.]

p.14. Legend FIG 1, line 2, after word 11, added '(arrows)'. Line 5, after word 10 'neocortex', added '(Cx ML, molecular layer of the neocortex)'. Line 6, after word 5 'cortex', added '(Cb GL, granule layer of the cerebellar cortex)'.

Manuscript IV

p. 11. Line 27, word 6 'Table 2', corrected to 'Table 4'.

p.12. Line 3, word 4 'Table 2', corrected to 'Table 3'.

p.15. Line 7, word 5 'Fig. 5A.', corrected to 'Fig. 5'. Line 9 'Fig. 4', corrected to 'Fig. 1'.

p.23. Table 3. Corrected '30 h' to '24 h' in 5 boxes.

p.26. Deleted line 5 Note g to Table 5.

p.26. Legend Fig. 3., line 7. Deleted word 2 and 3 'green: AQP4' and added 'Arrows: meningococci'.

p.27. Legend Fig 4., line 2 after 'granulocytes', added '(arrows) and intermingled'.

Line 2: deleted 'on the pial surface, b) Distinct clusters of'. Line 2, after 'Mc' added '(arrowheads)'. Line 3 and 4, added sentence: 'Note the pia mater (open arrows) and subjacent subpial edema (*).' Line 6, added 'small arrowheads'.

p.29. Figure 2. Added '+ light inflammation', '++ moderate inflammation' and '+++ severe inflammation' beneath picture A, B and C.

Manuscript V

p.15. Paragraph 3, line 2, corrected 'Figure 6' to 'Figure 5'.

p.21-23. Table 2-4. Corrected 'weight' to 'weight loss'. Substituted word 'overall condition' with 'PAS'. Table 2. Line 4, after word 5, added 'at 24 h or'. Row 5, column 4 and 5, added '5' and '7', respectively.

p.24. Legend Figure 3. Line 4, after word 5, added '(arrows)'. Line 5, after word 1, added '(*)'.

p.24. Legend Figure 3, revised sentence after D. to: 'The horse-radish peroxidase (HRP) precipitate was confined to large vessel walls (open arrows) and there was no leakage into the brain parenchyma through the capillaries (arrows).'

p.24. Legend figure 4. Line 6, word 1, corrected 'perivascular' to 'meningeal'.

4. LIST OF PAPERS

PAPER I
Wimolrat Puwarawuttipanit, April D. Bragg**, Didrik S. Frydenlund**, Maria N. Mylonakou, Erlend A. Nagelhus, Matthew F. Peters, Naiphinich Kotchabhakdi, Marvin E. Adams, Stanley C. Froehner, Finn-Mogens Haug, Ole Petter Ottersen and Mahmood Amiry-Moghaddam
Differential effect of α-syntrophin knockout on aquaporin-4 and Kir4.1 expression in retinal macroglial cells in mice
Neuroscience Volume 137, Issue 1, 2006, Pages 165-175

PAPER II
Didrik S. Frydenlund, Anish Bhardwaj, Takashi Otsuka, Maria N. Mylonakou, Thomas Yasumura, Kimberly G. V. Davidson, Emil Zeynalov, Øivind Skare, Petter Laake, Finn-Mogens Haug, John E. Rash, Peter Agre, Ole P. Ottersen, and Mahmood Amiry-Moghaddam
Temporary loss of perivascular aquaporin-4 in neocortex after transient middle cerebral artery occlusion in mice.
Proc Natl Acad Sci U S A. 2006 September 5; 103(36): 13532–13536

PAPER III
Didrik S. Frydenlund, Lisa Lunde, Øivind Skare, Petter Laake, Mahmood Amiry-Moghaddam
Dynamic changes in brain aquaporin-4 distribution in a mouse model of acute hyponatremia
Manuscript

PAPER IV
Tonje Davidsen, Cesilie G. Castellanos, **Didrik S. Frydenlund**, Ellen-Ann Antal, Stephan A. Frye, Laura M. A. Camassa, Erlend A. Nagelhus, Jan G. Bjålie, Ole P. Ottersen, Mahmood Amiry-Moghaddam and Tone Tønjum
Brain inflammation in wildtype and aquaporin-4 null mice in meningococcal meningitis model
Manuscript

PAPER V
Didrik S. Frydenlund*, Tonje Davidsen*, Cesilie G. Castellanos, Stephan A. Frye, Ellen-Ann Anthal, Laura M. A. Camassa, Erlend A. Nagelhus, Mahmood Amiry-Moghaddam, Ole P. Ottersen and Tone Tønjum
Brain water imbalance and aquaporin-4 expression in a mouse model for bacterial meningitis
*These authors contributed equally
Manuscript

5. INTRODUCTION

Water homeostasis is essential for normal brain function. In contrast to other organs, the brain is encased in a rigid skull. Thus, it cannot expand freely. Brain edema (net increase in brain water) is a life-threatening condition that calls for immediate action. Cerebral edema may increase intracranial pressure (ICP) and decrease cerebral perfusion, potentially leading to brain ischemia, herniation and death. Brain edema is associated with a plethora of medical conditions such as stroke, hyponatremia and meningitis; to name a few. Alas, the therapeutic options have not evolved significantly over the last eighty years and are still based mainly on surgical decompression or mannitol infusion (Bereczki et al., 2001; Jaeger et al., 2003; Bereczki et al., 2007). Needless to say, drilling through the scull is bound to be associated with bleeding and infections. The initial effect of mannitol administration is significant, but a rebound edema may occur because of leakage of mannitol into the brain parenchyma through a decaying blood-brain barrier. The current therapy does not target the molecular mechanisms that transport water in and out of the brain. Hence, there is an imminent need for novel therapeutic options. Thus, a molecular approach to the pathogenesis of brain edema was pursued in this thesis.

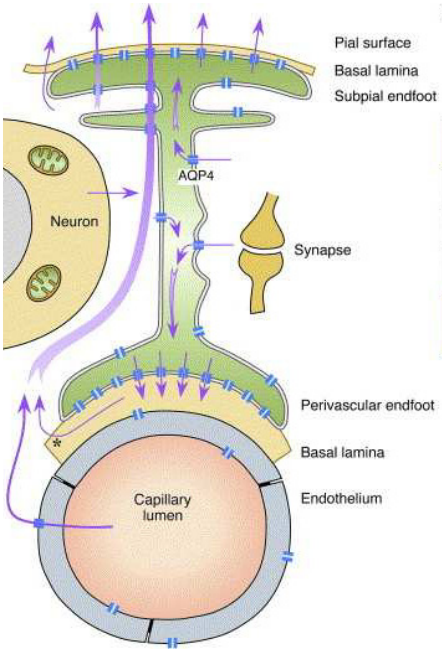

Fig 1. Schematic presentation of an astrocyte with aquaporin-4 water channels embedded in the plasma membrane. Arrows indicate hypothetic water fluxes in the brain (Amiry-Moghaddam et al., 2004a)

Water transport in brain: Hallmark of astrocytes

Astrocytes are highly polarized cells (Fig. 1). From the cell body, the astrocyte branches off with numerous processes. These processes abut onto nearby capillaries (the perivascular endfeet), the pia mater (the subpial endfeet) and the ependymocytes (the glia limitans interna).

All these endfeet are in contact with the brain-blood or brain-CSF interfaces.
Thus, the astrocyte is uniquely situated to be the key player in the regulation of water transport in the brain. A selective swelling of the perivascular endfeet is almost pathognomonic for some types of cerebral edema (Table 1). Astrocytes are endowed with a number of organic osmolytes (mainly amino acids) – and inorganic osmolytes (of which K^+ is the quantitatively most important). These can be released so as to temporarily counteract edema formation (Thurston et al., 1975; Sterns et al., 1993).

Table 1. Classification of brain edemas

Edema	Edema fluid	Mechanism	Clinical condition
Cytotoxic	Intracellular (glia)	ATP depletion Reversal of Na/K ATPase	Ischemia Toxins Meningitis?
Osmotic	Intracellular (glia)	Osmotic gradients	Hyponatremia The syndrome of inappropriate antidiuretic hormone hypersecretion (SIADH) Reversal of hyperglycaemia
Vasogenic	Extracellular	Disrupted blood-brain barrier	Brain tumors Prolonged ischemia Meningitis
Hydrocephalic	Extracellular	Decreased resolution of CSF and brain water	Hydrocephalus Meningitis?

When addressing brain edema, it is of paramount importance to know the distinction between the different classes of edema, because the pathophysiological mechanisms (and potential treatment) are very different. Cytotoxic (cellular) edema and vasogenic edema are the two classic types of edema as defined and investigated by the famous neuropathologist Igor Klatzo (Klatzo, 1987). Recently, further insight into the edema mechanisms has recognized osmotic- and hydrocephalic edema as distinct entities (Milhorat, 1992).

Recently, the discovery that a selective water channel (Aquaporin-4) is abundantly expressed in astrocyte endfeet has provided new insight into the molecular basis of water transport in the brain and instills hope for more efficient therapy

Emerging role of aquaporins in fluid physiology

Physiologists have long debated how large amounts of water are transported over cell membranes in cells or organs like erythrocytes and kidney as this transport exceeds severalfold what can be accounted for by simple diffusion.

The discovery that nearly every organ in the body is endowed with specific channels selectively transporting water has lead to a paradigm shift in our understanding of basic fluid physiology (Preston and Agre, 1991; Agre et al., 2002). To date, 13 mammalian members of the aquaporin family have been characterized. Each has a distinct cellular and subcellular localization. The mammalian aquaporins fall into three functional groups.

The first group compromises the true aquaporins, which are permeated by water only: AQP0, AQP1, AQP2, AQP4, AQP5 and AQP6 (Preston and Agre, 1991; Fushimi et al., 1993; Jung et al., 1994a; Mulders et al., 1995; Raina et al., 1995; Yasui et al., 1999b). However, AQP6 is a special case as its water permeability is increased at low pH and becomes permeable to urea, glycerol and anions if stimulated by mercury (Yasui et al., 1999a; Holm et al., 2004). Members of the second group, named the aquaglyceroporins, consist of AQP3, AQP7, AQP9 and AQP10 (Ishibashi et al., 1994; Ishibashi et al., 1997; Kuriyama et al., 1997; Ishibashi et al., 2002). They are permeable to water, ammonia, glycerol and urea (Rojek et al., 2008). AQP8 is a loner in the last group, the aquaammoniaporins, and is permeable to water and ammonia (Saparov et al., 2007).

The two last members AQP11 and AQP12, which were recently identified, belong to a new subfamily, the superaquaporins. They are still poorly characterized and little is known about their roles. However, AQP11 is proposed to be expressed in intracellular organelles (endoplasmic reticulum) in kidney tubules and in a subset of neurons and lacks water transport capacity (Gorelick et al., 2006). Unexpectedly, AQP11 null mice die before weaning, due to advanced renal failure with polycystic kidneys (Morishita et al., 2005). Finally, AQP12 is expressed intracellularly in pancreatic acinar cells (Itoh et al., 2005).

3D structural studies by X-ray crystallography studies have shown that AQP1 and other aquaporins are present as tetramers in the cell membrane (Walz et al., 1994). Unlike ion channels, the channel for water permeability does not reside at the centre of the tetramer. Instead, each of the four proteins of a tetramer contains a channel (Preston et al., 1993).

The hallmark of the monomeric structure of the aquaporin family is the three amino acid signature NPA (Asn- Pro- Ala) (Jung et al., 1994b). One NPA motif is found in the amino terminal half of each monomer, and a second NPA motif in the carboxy terminal half. The NPA motif is well conserved among the aquaporin family members (Park and Saier, Jr., 1996).

The selectivity of true aquaporins to water- excluding even hydronium ions - arises from three mechanisms. First, the channel narrows to a diameter of 3 Å which limits the size of molecules that can pass through it. A water molecule has a diameter of 2.8 Å (Murata et al., 2000). Secondly, two dipoles at the NPA motifs interact with each individual water molecule and prevent them from hydrogen bonding to adjacent water molecules (de Groot and Grubmuller, 2001). Finally, a positive charged residue (Arg-195) in the pore prevents cation flux (e.g. hydronium ions) (de Groot et al., 2001).

As for diffusion in general, the transport of water through aquaporins is dependent on an osmotic gradient across the membrane. Thus, aquaporins permit bi-directional water transport. Since the water transport depends on osmotic forces, there is no direct energy consumption involved in aquaporin mediated water flux.

Aquaporin-4 – the major aquaporin in brain

Aquaporin-4 (AQP4) is a water-selective channel originally characterized in 1994 and shown to be strongly expressed in brain (Jung et al., 1994a).
AQP4 is expressed primarily in astrocytes and is polarized in the perivascular endfeet around blood vessels and endfeet in contact with the pial surface, both brain-liquid interfaces (Nielsen et al., 1997). AQP4 is also expressed in the astrocyte membranes in the neuropil, albeit at a far lower concentration.

The AQP4 mRNA gives rise to two main isoforms: M1 (323 aa) and M23 (301 aa) (Jung et al., 1994a). The M23 isoform is by far the more abundant and is also more widely expressed

than M1 (Nielsen et al., 1997). Further, freeze-fracture analyses have revealed that M23 tetramers form orthogonal arrays of particles (OAPs), i.e., arrays of several tetramers clustered together (Verbavatz et al., 1997; Rash et al., 1998). The physiological implication of this peculiar arrangement of AQP4 is still elusive. M1 does not form OAPs alone.

Regulation of AQP4 expression

The short-term regulation of AQP4 expression has been shown to be dependent on endocytotic pathways and the action of several kinases (Verbavatz et al., 1997; Madrid et al., 2001; Gunnarson et al., 2008; Moeller et al., 2009). The dynamics of the AQP4 trafficking and recycling along the endocytic pathway *in vivo* in brain is currently unknown. In *Xenopus laevis* oocytes, activation of the vasopressin-receptor ($V1_aR$) and subsequent PKC dependent phosphorylation of serine 180 in loop D mediates increased internalization of AQP4 (Moeller et al., 2009). Interestingly, phosphorylation of serine 276 by casein kinase II has been shown to enhance AQP4 lysosomal targeting and degradation in epithelial MDCK cells (Madrid et al., 2001). In general, the regulation of AQP4 expression bears directly on the potential of AQP4 as a therapeutic target.

Glutamate excitotoxicity is proposed to play a pivotal role in the formation of postischemic cytotoxic edema. A proposed mechanism is that glutamate activates metabotropic glutamate receptors, causing Ca^{2+} release from intracellular stores, with a subsequent increase in $[Ca^{2+}]_i$. Calcium release activates calcium/ calmodulin-dependent protein kinase II (CaMKII) with subsequent phosporylation of serine 111 on AQP4 (Gunnarson et al., 2008). Glutamate did not increase water permeability in astrocytes lacking AQP4. Intriguingly, the effect of glutamate on water permeability in AQP4-expressing astrocytes also involves the NO signalling pathway, as the increase is abolished by applying inhibitors to NO synthases. AQP4 expression was not changed after glutamate exposure, and this begs the question if the decrease in water permeability is due to alterations in the structure of OAPs or single channel conformation (e.g. gating) (Gunnarson et al., 2008). However, the physiological relevance of AQP4 regulation is still obscure.

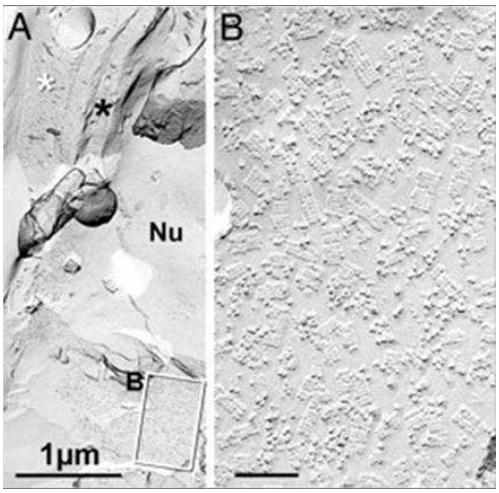

Fig.2 A) A low magnification image from the contact region between an astrocyte endfoot (white asterix) and the edge of a capillary (black asterix). Boxed area encloses astrocyte endfoot membrane. B) High-magnification view of astrocyte endfoot plasma membrane, showing numerous OAPs of AQP4 Modified from *Frydenlund et al. PNAS* 2006.

Aquaporin-4 multimerization

Several lines of evidence suggest that the M23 isoform assembles into OAPs in cell plasma membranes, whereas the full-length M1 isoform alone does not. A current hypothesis that has gained experimental support is that M1 may modulate the size of the OAPs. Thus, M23 alone forms very large OAPs, whereas M23 and M1 together form much smaller OAPs.

Recently, the molecular details for the dynamics of OAP formation have been elucidated. By employing the single particle tracking technique it has been shown that the M23 isoform is nearly stationary whereas the M1 isoform diffuses freely in the membrane (Crane et al., 2009b). Furthermore, single-channel water transport p(f) (cm/s) was found to be much greater for the M23 isoform (Silberstein et al., 2004). On the contrary, a recent analysis with the *Xenopus* oocyte assay found higher relative water permeability for the M1 isoform (Fenton et al., 2010).

In one study, expression of an M23 serine 111 mutant (S111E), mimicking the constitutive phosphorylation of this residue, produced approximately 1.5-fold greater single-channel p(f) and OAPs that were significantly larger than wild type M23 OAPs, suggesting that serine 111 may be involved in OAP formation (Silberstein et al., 2004).

Besides, it has been shown that two N-terminal cysteines of M1 are palmitoylated and this suggests that palmitoylation of the N-terminal cysteines is one of the reasons for the inability of M1 to form square arrays alone and that the hydrophobic residues in the N-terminus of M23 is important in array formation (Suzuki et al., 2008). Thus, deletion of the two cysteins (at position 13 and 17) in the N-terminus of M1 results in OAP formation, and furthermore, AQP1, which does not form OAPs, was induced to form OAPs upon replacement of its N-terminal domain with that of M23 (Crane et al., 2009a).

In conclusion, it seems that the formation of OAPs is highly regulated. The water flux through AQP4 may potentially be manipulated by interfering with the formation and dissolution of OAPs.

The polarization of AQP4 is a main focus of this thesis. The molecular basis for polarization of AQP4 in the perivascular endfeet has been characterized in some detail, and it has been resolved that AQP4 is anchored to the endfeet membranes through interaction with the dystrophin-associated protein complex (DAPC) (Fig 3.).

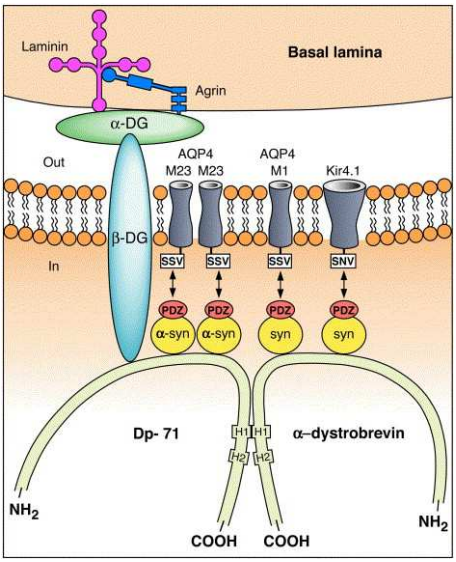

Fig. 3. Diagram showing the presumed molecular basis for the enrichment of AQP4 in the perivascular membrane (Amiry-Moghaddam et al., 2004a).

DAPC- the molecular basis for astrocyte polarization

The dystrophin-associated protein complex (DAPC) is a huge assembly of proteins expressed in several organs. The dystrophin gene is the biggest in the genome and localized on the X-chromosome. Mutations in the dystrophin gene lead to muscular dystrophies in male offspring. In Duchenne muscular dystrophy, there is a complete loss of dystrophin, but in Becker muscular dystrophy some aberrant dystrophin is usually transcribed and the phenotype is less severe (Hoffman et al., 1988). Several isoforms of dystrophin exist: The full length isoform (Dp427) is expressed mainly in skeletal muscle, whereas Dp71 is the main dystrophin isoform in astrocytes (Lederfein et al., 1992).

Several lines of evidence suggest that APQ4 is part of the DAPC in brain. *Mdx* mice is a strain arising from a spontaneous mutation in the dystrophin gene in inbred C57BL/10 mice (Bulfield et al., 1984). Thus, the mice lack dystrophin expression and interestingly also have perturbed expression of AQP4 (Liu et al., 1999). The perivascular expression of AQP4 in these mice is strongly reduced, while the total brain AQP4 levels assessed by immunoblots are unchanged.

α-Syntrophin is a scaffolding adaptor protein primarily expressed in skeletal muscle and astrocytes and an important contributor to the formation of the DAPC in brain (Adams et al., 1993). The C-terminus of α-syntrophin binds dystrophin, while the PDZ domain recruits other proteins to the dystrophin complex. The PDZ domains are found in many proteins and recruit molecules with a specific C-terminal sequence (SXV) into complexes (e.g. the synaptic PSD-95 complex) (Kornau et al., 1995).

APQ4 has a SSV sequence and interestingly, in a transgenic mice strain (Delta-PDZ) where α-syntrophin lacks the PDZ domain, AQP4 was absent from the sarcolemma (Adams et al., 2001). Prompted by this finding, Neely and co-workers showed that the polarization of AQP4 in the perivascular membrane was dependent on the expression of α-syntrophin (Neely et al., 2001). Thus, α-syntrophin null mice exhibited an almost complete loss of the perivascular pool of AQP4, but also in this case, the total amount of brain AQP4 was unchanged (Neely et al., 2001). However, pools of AQP4 independent of the DAPC and α-syntrophin exist. Such pools are found in astrocyte membranes in the neuropil of the granule cell layer in the cerebellum, in subpial membranes in the neocortex, and in the basolateral membranes of ependymal cells (Amiry-Moghaddam et al., 2004b; Nicchia et al., 2008). The molecular basis for polarization of AQP4 in these membranes is still enigmatic.

The insight in the molecular mechanisms underlying the polarized expression of AQP4 has provided a platform for the construction of transgenic mice and for the establishment of relevant models to assess APQ4 function.
The construction of AQP4 null mice or mice that have an altered expression pattern (α-syntrophin KO) has given valuable knowledge about the physiological and pathophysiological importance of AQP4 and has provided strong evidence that AQP4 is in fact an important player in several intracerebral pathologies.

The AQP4 null mouse model can be utilized to assess the global effect of knocking out all AQP4 pools in the brain (Ma et al., 1997). The α-syntrophin KO model, in contrast, is a selective and unique tool for assessing the functional importance of the AQP4 pool in the perivascular membrane (Adams et al., 2000).

Loss of astrocyte polarization in brain pathophysiology

Recently, evidence has accumulated to suggest that several disorders in the CNS are associated with a loss of glia polarization. An important goal is to unravel the pathophysiological impact of the concomitant redistribution of AQP4.

Role of AQP4 in neuronal excitability and epilepsy

The extracellular space (ECS) shrinks significantly upon neuronal depolarization (Dietzel et al., 1982). Hence, this could reflect water transport through the AQP4 pool that resides in perisynaptic astrocytic processes. Interestingly, the ECS is shown to *increase* in neuropil distant to the active synapses (Niermann et al., 2001). This provides us with a model where water uptake in one astrocytic membrane compartment is followed by a net efflux of water (reflected by an increase in ECS) in another membrane compartment. Mice lacking AQP4 have a slightly increased ECS (Binder et al., 2004b). Moreover, by recording cortical surface photobleaching of fluorescently labeled dextrans *in vivo*, it has been shown that extracellular diffusion of dextrans is faster in AQP4 KO animals than in WT controls (Binder et al., 2004b).

The inwardly rectifying potassium channel Kir4.1 is proposed to act in concert with AQP4 in the dynamic regulation of the ECS and in the setting of baseline ECS volume (Nagelhus et al., 1999). Further, this channel is responsible for a very negative membrane potential in astrocytes and is a key regulator of K^+ homeostasis, at least in glial Müller cells in retina. Here extracellular K^+ is taken up via Kir4.1 distally and siphoned through the pool of Kir4.1 in the subvitreal endfeet into the vitreous body, that acts as a sink (Karwoski et al., 1989; Kofuji et al., 2000). In conclusion, AQP4 might be involved in the dynamic regulation of the ECS. However, much more work is required to unravel the precise mechanisms underlying ECS volume control and the proposed interplay between AQP4 and Kir4.1 (Ostby et al., 2009).

Epilepsy is a major cause of morbidity worldwide. The neurobiological substrate for epileptic seizures is increased excitability in neurons, focally or globally.
The first direct evidence for a role of the perivascular AQP4 in epileptic seizures and the coupling between water flux and K^+ clearance was provided by Amiry-Moghaddam and co-workers (Amiry-Moghaddam et al., 2003b). Deletion of the perivascular pool of AQP4 by

α-syntrophin KO was found to delay clearance of K^+ following high frequency neuronal activation in acute hippocampal slices. Furthermore, mice lacking perivascular AQP4 exhibited more severe seizures than wild type animals when exposed to hyperthermia. It was proposed that the perivascular pool of AQP4 is coupled in series with the perisynaptic AQP4 pool and that both pools must be in place to ensure adequate K^+ clearance. Interestingly, one study found increased threshold for induction of seizures in APQ4 KO mice (Binder et al., 2004a). One possibility is that the increased seizure threshold reflects the increased ECS volume in AQP4 KO mice. Obviously, an increased ECS would serve to blunt the extracellular K^+ increase caused by neuronal activation. The role of AQP4 in epileptiform activity is still far from resolved, calling for further studies.

The experimental data suggesting a role of perivascular AQP4 in potassium and water homeostasis after neuronal depolarization, have partly been corroborated by clinical findings. Thus, in a severe form of epilepsy, the mesial temporal lobe epilepsy (MTLE), there is atrophy of neurons and astroglial changes in the hippocampus (Thom et al., 2009). Interestingly, the capacity for uptake of potassium after neuronal depolarization is decreased (Bordey and Spencer, 2004). Further, it was recently shown that the main dystrophin isoform in astrocytes (Dp71) is lost from the perivascular membrane, pointing to lost polarization of the glial endfeet. AQP4 is anchored to the DAPC and in MTLE the polarization of AQP4 is lost from the perivascular endfeet, whereas the total level of AQP4 was increased (Eid et al., 2005). This begs the question if the lost polarization of AQP4 is contributing to the pathophysiology and the reduced clearance of potassium.
However, a causal relationship remains to be established as the resected brain material studied was acquired from patients with fully developed epilepsy.

Brain tumor

Glioblastoma is a type of cancer that is feared due to its ability to diffusely invade the neighboring brain tissue and its proneness to induce brain edema and hernation. Alas, the treatment options are limited. Radical surgery with severe side effects may prolong the survival for some months, but the patient will inevitably succumb in the end.
In glioblastomas there is a substantial loss of astrocyte polarization. Hence, AQP4 and α-syntrophin are redistributed from the perivascular membrane to the entire surface of the astrocyte (Warth et al., 2004). The molecular substrate for the loss of polarization in

glioblastomas is not known but inflammation and proteolysis of the perivascular basal lamina (responsible for anchoring the dystrophin complex) might play a role.

Several lines of evidence suggest that the integrity of the DAPC is contingent on interaction between dystroglycans in the astrocyte and extracellular matrix (ECM) molecules as agrin in the basal lamina (Ibraghimov-Beskrovnaya et al., 1992). Hence, the activity of matrix metalloproteinases (MMPs) is significantly increased in gliomas, and MMPs have several ECM components (such as agrin and laminin) as substrates (Galloway et al., 1983; Rao et al., 1993).

The lost polarization is likely to have pathophysiological relevance. AQP4 helps increase taxis of cells by increasing their ability to undergo dynamic volume changes and hence their ability to navigate in the tortuous extracellular space (Auguste et al., 2007). Indeed, inhibition of PKC in gliomas reduced AQP4 phosporylation and significantly enhanced tumor invasion (McCoy et al., 2010).

Cerebral stroke

Stroke is the third leading cause of death and a major cause of disability in the industrialized world (Lloyd-Jones et al., 2009). The incidence is expected to sky-rocket as the population ages.

Again, therapeutic options are limited. Promising candidate targets from animal experiments have disappointed in human clinical trials. Tissue plasminogen activator (tPA) has been shown to be beneficial, however, the risk of bleeding is significantly increased so the time-window has been limited to patients with a symptom debut less than 4 ½ h prior to admission (Schellinger et al., 2004). Thus, only 2-3 percent of stroke patients receive tPA and the clinical usefulness is therefore still limited.

Particularly challenging are thrombotic strokes in the inlet of the middle cerebral artery.
In early stroke pathophysiology, the brain area where blood flow is either absent or measures less than 10 ml/100 g brain tissue/min is rapidly and irreversibly damaged in less than 6 minutes, forming an ischemic core. This infarcted tissue is surrounded by a border zone of hypoxic, but living tissue with blood flow greater than 20 ml/100 g brain tissue/min. Cells in the border zone undergo cytotoxic edema and other changes that are potentially reversible if

perfusion is restored within the first few hours after injury. If not, the cells with cytotoxic edema will inevitably die and extend the area with cell death deeper into the parenchyma than the original core (Simard et al., 2007). Hence, the cells in the border zone are the main therapeutic target in the prevention of ischemic stroke and injury.

With manifest infarction there is also a gradual increase in vasogenic edema, but this may take hours to days. The activation of matrix metalloproteinases is a key event in the inflammation associated with stroke and has been shown to contribute to the formation of vasogenic edema, by proteolytic degradation of the basal lamia separating the capillary from the endfoot (Rosenberg et al., 1996).

Recent analyses revealed that the integrins are lost and the astrocyte endfoot detached from the basal lamina soon after onset of ischemia (Tagaya et al., 2001; Kwon et al., 2009). This may affect astrocyte polarization and contribute to the pathophysiological events.

Emerging role of AQP4 in meningitis and brain edema

Bacterial meningitis is an inflammation of the meninges affecting the pia, arachnoid and subarachnoid space that occurs in response to bacteria and bacterial products. Meningitis continues to be an important cause of mortality and morbidity in neonates and children worldwide (Chang et al., 2004).

AQP4 and bacterial meningitis

Bacterial meningitis is still after three generations of the availability of efficient antibiotics a major cause of death and disability in children and youngsters worldwide (Lin and Safdieh, 2010). The majority of cases of acute bacterial meningitis are caused by the mucosal opportunistic pathogens *Streptococcus pneumoniae* (the pneumococcus, *Pc*)*, Neisseria meningitidis* (the meningococcus, *Mc*) and *Haemophilus influenzae* (Davidsen et al., 2007). The vaccine against *H. influenzae* type B (Hib) given to children as part of their routine immunizations has dramatically reduced the occurrence of serious *H. influenzae* disease. Currently, vaccines against major serogroups of Pc and Mc are available.
However, a vaccine against Mc serogroup B is not yet available (Tonjum, 2005; Davidsen and Tonjum, 2006).Today, *N. meningitidis* and *S. pneumoniae* are the leading causes of bacterial meningitis.

Even though the seriousness of *S. pneumoniae* and *N. meningitidis* infection is well known, the exact interplay between microbe and host is still elusive (Davidsen and Tonjum, 2006; Weber and Tuomanen, 2007; Orihuela et al., 2009). This has impeded the development of new therapeutic options based on an understanding of the molecular pathogenesis (Davidsen et al., 2007). Undoubtedly, antibiotics can be lifesaving, however, the inflammatory cascade persists after the start of treatment due to release of antigenic components from decaying bacteria, potentially leading to brain edema. This may ultimately cause increased intracranial pressure and in fatal cases herniation and death of the patient. Cerebral herniation occurs in about 5% of patients with acute bacterial meningitis, accounting for about 30% of the mortality (Joffe, 2007). Corticosteroids are recommended as an adjuvant to antibiotics in the treatment of pneumococcal meningitis to reduce the host inflammatory response and secure the integrity of the blood-brain barrier (Koedel et al., 2010). Recent animal experiments have shown increased apoptosis in the hippocampal formation that could question the usefulness of corticosteroids in the clinic (Leib et al., 2003).

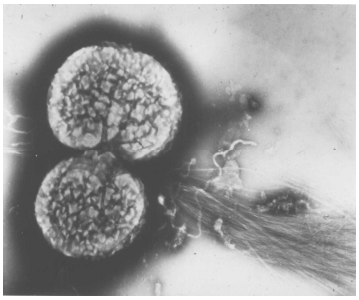

Fig. 4. EM image of piliated *N. meningitidis* H44/76 wildtype strain (Tønjum, 2005)

N. meningitidis, a Gram-negative diploccous, is a strict human pathogen and is also commonly a constitutive part of the normal upper airway flora (Tonjum, 2005; Davidsen et al., 2007; Weber and Tuomanen, 2007). The pathogenesis of *N. meningitidis* is contingent on several virulence factors (Nassif, 2000; Tonjum, 2005). The key virulence factor is the production of a polysaccharide capsule shown to mediate protection against phagocytic killing, opsonization and complement-mediated killing (Goldschneider et al., 1969a; Goldschneider et al., 1969b). Of prime importance for virulence are the long, polymeric

structures emanating from the bacterial surface, as they are a prerequisite for adherence and infection. The bacteria also express an IgA_1 protease, increasing the ability to thrive on mucus membranes. Thus, *N. meningitidis* is partly protected from the immune system.

Occasionally, *N. meningitidis* may transverse the epithelium by transcytosis and enter the bloodstream (Stephens et al., 2007). Bacteremia may develop into full blown sepsis or the bacteria may adhere to brain capillaries and then subsequently pass through the blood-brain barrier, ultimately causing meningitis. However, the mechanism of meningococcal invasion and passage through the mucosa and blood-brain barrier is only partially known. Filamentous appendages (type IV pili) (Fig. 3.) are a prerequisite for adherence to the mucosal and capillary surfaces (Pujol et al., 1999). Interestingly, bacteria isolated from blood or the cerebrospinal fluid (CSF) of patients with sepsis and meningitis are heavily encapsulated, suggesting that capsule formation is a key step in the transition from the nasopharyngeal state to invasive CNS disease (Nassif, 2000).

Lipooligosaccharide (LOS) in the outer membrane is a potent activator of TLR4 on meningeal macrophages, astrocytes and microglia. The subsequent release of cytokines (i.e. TNF-α/ IL-1) attracts circulating granulocytes and monocytes into the CSF. As they lyse, granulocytes and monocytes release powerful lysosomal enzymes and free radicals, which may ultimately lead to disruption of the blood-brain barrier.

S. pneumoniae is an alpha-hemolytic, Gram-positive bacterium which has several disease manifestations; the most important ones being pneumonia, otitis media and meningitis.
The capsule is the major virulence factor of *S. pneumoniae*, as the non-encapsulated strains are only barely pathogenic (Avery and Dubos, 1931; Watson and Musher, 1990). Other key virulence factors are cell wall components (peptidoglycan) and pneumolysin.
As *S. pneumoniae* is a naturally virulent pathogen in mice, this pathogen has been studied in several mouse models for experimental bacterial meningitis (Chiavolini et al., 2004; Orihuela et al., 2009).

Currently, there seems to be uncertainty as to the mechanisms and prevalence of brain edema in meningococcal meningitis. This can partly be attributed to the diverse disease manifestations of meningococcal meningitis, such as disseminated intravascular coagulation,

thrombosis, vasculitis, and parenchymal inflammation with possible abscess formation (Bauserman and Naul, 2003; Stephens et al., 2007).

After the inflammation in meningitis has subsided and the bacteria have been eradicated, a thick fibrinopurulent exudate in the subarachnoid space may organize into fibrous tissue that blocks the exits of the fourth ventricle and impairs CSF circulation around the cerebral convexities (Koedel et al., 2010). This may lead to manifest postinfectious hydrocephalus. Other frequent sequela are deafness and epilepsy (Pumain and Heinemann, 1985; Edmond et al., 2010).

In a recent study, *S. pneumoniae* was infused into the basal cisterna of CD1 mice (Papadopoulos and Verkman, 2005). The mice developed brain edema, with a very high mortality. However, CD1 outbred mice lacking AQP4 had a tremendous reduction in edema formation and mortality. Based on the facts that perivascular endfeet were swollen, tight junctions were intact, and diffusion was reduced in the intercellular space, the authors concluded that the primary edema was likely to be cytotoxic. AQP4 was reported to be up-regulated 7-fold in the neocortex of wild type mice, following S. pneumoniae infusion. In another study, intracerebrospinal administration of IL-1β in otherwise non-manipulated mice led to a significant upregulation of AQP4 (Ito et al., 2006). Interestingly, inhibition of the nuclear factor-κB pathway abolished the induction of AQP4. Although intriguing findings, the exact mechanisms for this extreme increase in AQP4 are at present obscure. However, the potential for targeting AQP4 in the treatment of pneumococcal meningitis is obvious (Papadopoulos and Verkman, 2008).

AQP4 could potentially be a key player in brain edema formation in meningococcal meningitis as well. However, the cell wall components of *S. pneumoniae* (peptidoglycan and teichoic acid) and the outer membrane lipopolysaccharide of *N. meningitidis* (LOS) partly activate different cascade systems, in addition to the common effect through IL-1. Thus, the potential role of AQP4 in brain edema formation in meningococcal meningitis is *a priori* difficult to predict.

Despite this serious challenge, animal models of meningococcal meningitis are few and a valid model has yet to be established in mice. In order to benefit from the ever-increasing number of transgenic mice strains available, including a transferrin-overexpressing iron-

binding strain it is of paramount importance to establish a valid mouse model for meningococcal meningitis (Zarantonelli et al., 2007).

AQP4: specific role in brain edema formation and resolution

AQP4 holds a strategic position at the brain-fluid interfaces, pointing to AQP4 as a key player in brain water transport. The pathophysiological importance of AQP4 has been elucidated in several mouse models of brain edema.

Cytotoxic and osmotic edema

Cytotoxic edema

A pioneer study revealed the effect of AQP4 KOs on outcome in a model of ischemic stroke (Manley et al., 2000). The MCAO model is based on temporary occlusion of the middle cerebral artery by a nylon filament for 90 min followed by reperfusion. 24 h after ischemia followed by reperfusion transgenic mice lacking AQP4 showed dramatically reduced brain edema formation and increased survival.

Moreover, α-syntrophin KO mice developed less edema than WT controls after MCAO (Amiry-Moghaddam et al., 2003a). Serial brain sections were treated with triphenyltetrazolium chloride (a mitochondrial stain) to differentiate between infarcted and non-infarcted tissue. Interestingly, the infarction core was reduced in α-syntrophin KO mice.

Osmotic edema

Hypotonic hyponatremia is associated with a wide range of conditions, e.g. endocrine disorders, renal- and heart failure; all adversely affecting the water and electrolyte balance in the brain (Sonnenblick et al., 1993; Hanna and Scanlon, 1997; Adrogue and Madias, 2000; Moritz and Ayus, 2007). Hyponatremic edema may also be iatrogenic (too extensive use of diuretics or hypotonic fluids).

The decrease in brain osmolality will inevitably set up an osmotic gradient forcing water into the brain. Intriguingly, the survival and outcome after acute hyponatremia produced by intraperitoneal water infusion were greatly improved in both AQP4 KO and α-syntrophin KO mice (Manley et al., 2000; Amiry-Moghaddam et al., 2004b).

Vasogenic and hydrocephalic edema

We now have a large quantity of experimental data from AQP4 null mice in models for vasogenic and hydrocephalic edema, such as cortical freeze injury, brain tumor, brain abscess and hydrocephalus (Papadopoulos et al., 2004; Bloch et al., 2005; Bloch et al., 2006).

Vasogenic edema

In one study, *Staphylococcus aureus* was injected into the striatum to create a focal abscess (Bloch et al., 2005). The immune response was similar in wild type and AQP4 null mice. The disruption of the blood-brain barrier is probably secondary to the infectious process with release of cytokines and bacterial components into the neuropil. The disruption of the blood-brain barrier was similar in both groups, assessed by extravasation of Evan's blue. At day 3 the AQP4 mice had significantly increased intracranial pressure and brain water content compared with the controls.

The edema following the expansion of a brain tumor may increase the ICP and aggravate the neurological deterioration. In astrocytomas, AQP4 is massively up-regulated as judged by non-quantitative immunolabelling and the polarization of AQP4 is lost. Hence, AQP4 is distributed evenly over the astrocyte membrane. Moreover, increased AQP4 expression is seen in reactive astrocytes around metastases of adenocarcinomas (Saadoun et al., 2002).
In a mouse model of brain tumor edema, melanoma cells were implanted stereotactically and allowed to grow in the brain parenchyma. After 7 days there was greater elevation in ICP and more severe neurological deterioration in the AQP4 null mice than in wild type controls, most likely due to an impaired removal of brain water (Papadopoulos et al., 2004). Thus, AQP4 may be an important modulator of edema resolution in aggressive primary brain tumors as well as metastases. The phenotypic impact of AQP4 gene deletion is in line with the studies suggesting that the CSF may act as a sink for excess brain water so as to counteract brain edema formation (Hochwald et al., 1976). Hence, AQP4 may contribute to the sink function of the CSF by its presence in the brain-CSF interfaces.

Hydrocephalic edema

In a model of non-communicating hydrocephalus, kaolin was infused into the cisterna magna with a subsequent obstruction of the transport of CSF into the subarachnoid space (Bloch et al., 2006). In this model, AQP4 null mice showed a more rapid increase in brain edema and ICP, yielding a more extensive neurological impairment than the wild type controls. These

findings corroborate the proposed role of AQP4 in mediating efflux of CSF when the normal drainage routes are compromised, and possibly also under normal physiological conditions.

To sum up, it turns out that AQP4 has multifarious roles in the pathophysiology of brain edema. In cytotoxic and osmotic edema, AQP4 is likely to increase development of brain edema. AQP4 could increase the influx of water through the perivascular membrane directly by increasing the permeability coefficient of the blood-brain barrier, but this theory is tempered by the fact that there are presently no known aquaporins in the endothelial cells. In ischemia and osmotic edema, a plausible explanation is that AQP4 increases the kinetic of the swelling associated with sodium accumulation (cytotoxic) or water (osmotic) and setting up a new osmotic gradient forcing water into the brain. However, the possibility remains that AQP4 modulates the flux of water through hitherto unknown mechanisms.

In vasogenic and hydrocephalic edema, AQP4 is likely to increase the resolution of brain edema by facilitating bulk flow of water through the subpial membrane (maybe also the perivascular membrane) and the ependymal lining into the subarachnoid space and ventricles. These spaces could act as sinks and help shunt fluid out of the cranial cavity through the arachnoid villi. The exact magnitude of bulk flow through these endfeet is currently unknown.

In conclusion, the use of transgenic mice has been crucial in unraveling the pathophysiological importance of AQP4 in several models of brain edema.

However, the temporal dynamics and regulation of AQP4 *in vivo* in different membrane domains in edema formation and other pathologies are largely unexplored. Thus, it is of paramount importance to gain further insight into these issues before considering AQP4 a candidate for therapeutic intervention.

6. HYPOTHESES AND AIMS OF THE STUDY

AQP4 has a Janus-phased role in brain edema formation, where the pools of AQP4 in different membrane domains are likely to have divergent roles in brain edema formation and resolution. Hence, we hypothesized that AQP4 must be subject to regulation in CNS disease associated with the development of brain edema to 1) decrease the influx of water into the brain and 2) increase the efflux of water out of the brain so as to enhance resolution of brain edema. Consequently, we hypothesized that AQP4 has separate roles in different membrane domains and that these polarized pools of AQP4 will respond differently to osmotic gradients and edema formation and must be subject to local regulation.

Finally, we hypothesized that local differences in anchoring mechanisms are likely to influence polarized AQP4 expression and distribution during pathogenesis.

To unravel the dynamics of AQP4 expression in different membrane domains and the impact of AQP4 on brain edema formation in CNS pathogenesis, we have utilized different clinically relevant models with edema formation. More specifically; the subgoals to advance our knowledge and challenge our hypotheses were:

I. To unravel the mechanisms responsible for the polarized expression of AQP4 in retinal macroglial cells.

II. To elucidate the effect of transient ischemia on AQP4 expression and distribution in the perivascular endfeet in different brain regions in the infarction core and border zone after various reperfusion times.

III. To explore the polarization and distribution of AQP4 in different brain regions and membrane domains after induction of hyponatremia.

IV. To develop a mouse model for bacterial meningitis, suitable for unraveling the role of AQP4 in meningococcal meningitis.

V. Use this model to investigate the expression of AQP4 in whole brain and different membrane domains and the effect of AQP4 deletion on brain edema formation and pathogenesis in meningococcal meningitis.

7. RESULTS AND CONCLUSIONS

Paper I

Differential effect of alpha-syntrophin knockout on aquaporin-4 and Kir4.1 expression in retinal marcoglial cells in mice.

The expression of AQP4 in the perivascular endfeet in brain is dependent on α-syntrophin, as less than 10% of perivascular AQP4 remained in α-syntrophin KO mice. Thus, we wanted to investigate if another part of the CNS, the retina, displayed similar anchoring mechanisms and also to generate new hypotheses about anchoring of AQP4 and Kir4.1.

In the retina, the expression of AQP4 was higher in the perivascular membranes, than subvitreally, indicating enrichment in the former membrane domain.
Deletion of the α-syntrophin gene caused a significant loss (70%) of AQP4 in the perivascular and subvitreal membrane, as judged by quantitative analysis of the linear gold particle density. In wild type animals, the labeling of Kir4.1 was more intense in endfeet membranes than other membrane domains. Moreover, there was no reduction in the Kir4.1 labeling intensity in α-syntrophin KO mice. On the contrary, the perivascular membrane domains showed a statistically significant increase in Kir4.1 immunolabeling following gene deletion of α-syntrophin.

With the use of selective antibodies, we were able to show that another member of the syntrophin family, β1-syntrophin, is heavily expressed in the perivascular and subvitreal membranes of both wild type and α-syntrophin KO mice. Finally, deletion of α-syntrophin did not cause any up- or downregulation of β1-syntrophin.
We conclude that in the retina, the polarized anchoring *of AQP4, but not Kir4.1, is dependent on α-syntrophin.*

Paper II

Temporary loss of perivascular aquaporin-4 in neocortex after transient middle cerebral artery occlusion in mice.

Ischemic stroke is the third leading cause of death and the concomitant brain edema contributes by increasing the intracranial pressure and making the patient vulnerable to herniation. As the ischemic event progresses, the astrocytes become unable to regulate ionic gradient that is crucial in glial physiology. Hence, uptake of water via AQP4 in the perivascular endfeet will inevitably yield a cytotoxic edema. Thus, we wanted to explore the effect of ischemia on the α-syntrophin dependent perivascular pool of AQP4 (paper I and (Amiry-Moghaddam et al., 2003a) in the infarction core and the less affected border zone.

By utilizing a well established stroke model in mice (MCAO) it was found by quantitative immunogold cytochemistry that the ischemic striatum and neocortex show distinct patterns of AQP4 expression in the reperfusion phase after 90 min of middle cerebral artery occlusion. The striatal core displayed a loss of perivascular AQP4 at 24 h of reperfusion with no sign of subsequent recovery. The most affected part of the neocortex also exhibited loss of perivascular AQP4, but showed a tendency towards recovery at 72 h of reperfusion.
The cortical border zone differed from the central part of the ischemic lesion by showing no loss of perivascular AQP4 at 24 h of reperfusion, but rather a slight increase.

Theoretically, the remarkable reduction in the immunosignal could be due to conformational changes in the AQP4 protein, decreasing the antigenity of the epitope.
This possibility was ruled out by employing freeze fracture electron microscopy where the perivascular membrane of the infarction core showed a dramatic reduction of OAPs.
We then investigated if also α-syntrophin was downregulated or redistributed in ischemia. However, the α-syntrophin labeling in the perivascular membrane was intact in the infarction core and therefore not compatible with a general disruption of perivascular plasma membranes. Thus, the interaction between AQP4 and α-syntrophin seems sensitive to severe ischemia as the expression of AQP4 was largely unchanged in the less affected border zone.
We conclude that the size of the AQP4 pool in the perivascular membrane
is subject to *large and region-specific changes in the reperfusion phase*.

Paper III

Dynamic changes in brain aquaporin-4 distribution in mouse brain after induction of hyponatremia

Having explored the dynamics of AQP4 in ischemia with subsequent reperfusion in paper II, we wanted to explore more selectively the impact of edema on the expression of AQP4 in different domains and with different anchoring mechanisms (cf. hypotheses above). Hyponatremia will inevitably create an osmotic gradient between blood and brain. Thus, this condition is uniquely relevant for studying the impact of an osmotic gradient change on AQP4 distribution.

An electron microscopic analyis of mice sacrificed after acute induction of hypotonic hyponatremia (HN) revealed striking differences in 1) AQP4 immunolabelling between the neocortex and the cerebellar cortex and 2) immunolabelling in different membrane domains within the same brain region.

Notably, the neocortex demonstrated a significant increase (64%) in the labelling in the subpial membrane after 20 min HN that was followed by a significant drop (41%) in the labelling after 120 min HN. At 4 h after onset of hyponatremia an immunoblot analysis revealed that the protein levels of AQP4 was reduced significantly in the superficial parts of the neocortex, while no changes where observed in the deeper layer or at earlier time points. However, in the cerebellar cortex the density of gold partices was increased (by 44%) in the astrocyte membranes in the neuropil in the granule cell layer after 45 min HN. Strikingly, the astrocytic membrane in the neuropil in the granule cell layer had significantly less labelling (23%) after 120 min compared with 45 min HN.

We conclude that the immunoreactivity of AQP4 is *heavily dependent on brain region, membrane domains and time course after induction of hyponatremia.*

Paper IV

Brain inflammation in wildtype and aquaporin-4 null mice in meningococcal meningitis model

Prompted by the results from the two functional studies, we decided to look at AQP4 expression in yet another model with concomitant edema, namely meningococcal meningitis. However, in the absence of a suitable model for meningococcal meningitis, we were forced to develop our own.

AQP4 has been reported to be massively upregulated in pneumococcal meningitis (Papadopoulos and Verkman, 2005). We established a model to study the impact of meningitis on AQP4 expression and also the impact of AQP4 on the water balance in meningococcal meningitis.

Three mice strains (CD1, C57BL/6 and AQP4 null mice in a C57BL/6 genetic background) were subjected to intra-cerebrospinal fluid (CSF) injection of *N. meningitidis* serogroup B or PBS as a negative control. Some mice were injected with *S. pneumoniae* or lipooligosaccharide (LOS).
An electron microscopic analysis showed massive infiltration of granulocytes on the pial surface. There was focal clustering of meningococci attached to the pial surface.
Further, the mice showed sign of sickness as locomotion was decreased considerably. The expression of *Tnf-α* was increased severalfold as a sign of severe inflammation.

In mice with Mc the *Tnf-α* expression levels were increased after 9 hours, predominantly in the core brain, but after 30 h the inflammation was mostly confined to the brain surface and locomotion in these mice was also severely reduced. However, in Pc animals *Tnf-α* was increased in the brain surface at 9 and 24 h. In LOS injected mice, *Tnf-α* was increased at the brain surface and in core brain at 9 h. On the contrary, at 30 h *Tnf-α* was increased predominantly in the core brain. The neuropathological assessment of mice injected with PBS, Mc, Pc or LOS revealed that in general there was a correlation between brain inflammation by histopathology, high *Tnf-α* gene expression and reduced locomotion.

We conclude that the mice in this model infected intracisternally with *N. meningitidis*, develop clinical meningitis that shows resemblance with the pathogenesis in humans.

Paper V

Brain water imbalance and aquaporin-4 expression in a mouse model for bacterial meningitis

Here we utilized the model in paper IV to first gain insight into the brain edema formation in this model and then investigate the expression of AQP4 in meningococcal meningitis.

In CD1 mice there was a significant increase in brain water 24 h after injection of meningocci. Surprisingly, C57BL/6 mice injected with Mc did not have increased brain water. Unexpectedly, 24 h after injection brain water was increased significantly in AQP4 KO mice infected with Mc, compared with AQP4 KO mice injected with PBS.

Prompted by this, we decided to explore the effect of strict temperature control on brain water formation. Intriguingly, brain water was now significantly increased in C57BL/6, thus, pointing to an effect of temperature on edema development in meningococcal meningitis. Yet again, the brain water in *AQP4* null mice infected with Mc was increased more than in the other mice strains, displaying a massive 1% increase in brain water.

As AQP4 was reported to be tremendously increased in a previous work in mice infected with *S. pneumoniae,* we undertook a thorough analysis of AQP4 protein and gene expression in mice infected with Mc or Sp. However, none of our analyses showed any signs of upregulation of AQP4 in meningococcal or pneumococcal meningitis.

Thus, the gene expression of *Aqp4* seemed to be unaltered or only modestly changed in Mc and Pc meningitis. Interestingly, however, the gene expression *of Aqp4* was increased severalfold (4 x) in the core brain at 9 and 30 h in the mice with LOS injection as compared to the negative controls. Our immunoblot analysis revealed that AQP4 was decreased in mice infected with *N. meningitis* for 24 h (36%) and *S. pneumoniae* for 30 h (44%, $P < 0.03$).

We conclude that the brain water is increased, in a temperature-dependent manner and mice lacking AQP4 accumulate more brain water than wildtype mice in meningococcal meningitis.
Finally, the AQP4 expression is not increased in Mc or Pc mice, but seems on the contrary to be modestly downregulated in mice infected with *N. meningitidis* or *S. pneumoniae*.

8. DISCUSSION

8.1 Impact of results

The present study has provided new insight into the dynamics of AQP4 in pathophysiology. We have shown that AQP4 pools in different parts of the brains and in specific membrane domains display unique expression patterns and are presumably subject to local regulation in pathophysiology (cf hypotheses).

α-Syntrophin dependent anchoring of AQP4 in retina

We have previously shown that AQP4 is dependent on α-syntrophin for its anchoring in the perivascular endfeet in the brain (Neely et al., 2001).

In the retina our results revealed that AQP4, but not Kir4.1, is dependent on α-syntrophin for its anchoring in the subvitreal or perivascular membrane, displaying a ~70% decrease in the α-syntrophin KO mice. However, there is possibly a pool of AQP4 that is insensitive to α-syntrophin gene deletion, as the dependency of α-syntrophin in the perivascular membranes in brain is over 90%. Moreover, we also found strong expression of β_1-syntrophin in the aforementioned membrane domains and it is tempting to speculate that β1-syntrophin could be responsible for the proposed α-syntrophin independent pool in the perivascular – and subvitreal membranes in the retina. Our findings are partly corroborated by studies with Dp71 KO mice, lacking the main glial dystrophin isoform, where AQP4 is redistributed and the expression markedly reduced in the retina, whereas the expression of Kir4.1 is unchanged (Dalloz et al., 2003; Fort et al., 2008). However, α-syntrophin expression was unchanged, thus not directly dependent on Dp71 for its expression in the retina.

If α-syntrophin is unchanged why is AQP4 reduced if dependent on α-syntrophin (present study)? Biochemical analysis has given some clues as α-syntrophin is unable to pull down AQP4 without a cross-linker (Neely et al., 2001). Thus, the interaction is probably dependent on an intermediate molecule (here called protein X).

The expression and anchoring of protein X should be dependent on the coexpression of Dp71 and α-syntrophin. Thus, in Dp71 KOs the loss of interaction between Dp71 and α-syntrophin could destabilize protein X and AQP4 and *vice versa* with the α-syntrophin KOs.

In the Dp71 KOs utrophin, a homolog to dystrophin, was increased severalfold, indicating that α-syntrophin may interact with utrophin in the absence of Dp71, as utrophin has strong affinity to α-syntrophin in biochemical analysis (Fort et al., 2008).

We have previously hypothesized that Kir4.1 and AQP4 may act in concert in the uptake of water and potassium after neuronal depolarization. Our functional analyses of the α-syntrophin KO model could be seriously confounded if Kir4.1 was massively dislocated from the perivascular membrane, along with AQP4.

In our study we did not distinguish between the Müller cell endfeet and the astrocyte endfeet processes. Neither did we distinguish between capillaries in different layers of retina. We can not rule out that the syntrophin dependency of AQP4 or Kir4.1 differs between cell types (Müller cells vs. astrocytes) or between retinal layers.

AQP4 undergoes major changes after ischemic stroke

In paper II we demonstrated that the α-syntrophin dependent perivascular pool of AQP4 is temporarily lost after middle cerebral artery occlusion (MCAO).

These findings bear on the molecular mechanisms underlying the generation and resolution of postischemic edema. Since AQP4 in the perivascular membrane allows bidirectional water flow, this pool is likely to be rate limiting for water influx as well as efflux. In the early ischemic event, the edema mechanism is largely cytotoxic. Later, disruption of the blood-brain barrier will lead to development of vasogenic edema. Thus, the initial downregulation of the perivascular pool should be beneficial in the early event and impede influx, while later in the time course the partial recovery of AQP4 expression would be expected to favor the resolution of the edema.

Our conclusion is that the loss of AQP4 immunogold signal from perivascular membrane reflects a loss of AQP4 molecules from these membranes. Alternatively, the observed reduction in AQP4 immunolabelling could be due to conformational changes of the epitope, reducing its affinity to the antibody. One must also consider the possibility that the reduction in the immunosignal is non-selective and caused by a general disruption of the astrocytic plasma membranes in the postischemic phase. Both of these alternative explanations can be ruled out by supportive experiments.

Notably, in collaboration with Dr. John Rash and coworkers we were able to demonstrate a clear reduction in the number of perivascular orthogonal arrays (OAPs) in the infarction core at 24 h of reperfusion. This is consistent with loss of AQP4 rather than changes in the conformation of this molecule. Further, our finding of persistent α-syntrophin labeling in the perivascular membrane is not compatible with a general disruption of perivascular plasma membranes.

We do not know the mechanisms that underlie the postischemic loss of AQP4. A plausible explanation is that the coupling between AQP4 and α-syntrophin is sensitive to ischemia. Thus, changes in the microenvironment (e.g. acidification, calcium influx or oxidative processes) may weaken the affinity between these two molecules. Following disruption of its anchoring, AQP4 would diffuse laterally in the astrocytic plasma membrane. As the perivascular membrane is small compared to the total astrocytic surface the loss of AQP4 from endfoot membranes will not necessarily lead to a detectable increase in the AQP4 labelling in non-endfoot membranes

The MCAO model reveals pronounced differences between the cortical and striatal parts of the infarcts when it comes to the changes in AQP4 expression after MCAO. These differences probably reflect the fact that striatum is more severely affected than the cortex following ligation of the middle cerebral artery. This is also consistent with clinical findings. The observation that the perivascular pool of AQP4 is lost in the infarction core could at first sight seem disappointing as one might argue that this will reduce the usefulness of AQP4 as a potential target. However, the target for modern stroke therapy is primarily in the border zone, where most of the cells are viable, but in a dormant state. AQP4 is not downregulated in the border zone, rather there is a tendency towards upregulation. Blockage of AQP4 in the border zone of the infarcted area could very well decrease the secondary water influx associated with cytotoxic edema and thus the size of the infarction core. Immediate action with blockage of AQP4 could also minimize the infarction core.

Dynamic and membrane-specific changes of AQP4 in hyponatremia

In paper III we explored the influence of osmotic gradient on AQP4 distribution in different parts of the brain and membrane domains in a mouse model of acute hyponatremia.

Our results show that the neocortex responds to hypotonic hyponatremia by a short-term upregulation in the subpial membrane, while in the cerebellar cortex there is an upregulation in the granule cell layer. These changes are short lasting as there is reduced immunoreactvity for AQP4 after 120 min HN in the same membranes. An immunoblot analysis showed no differences in AQP4 immunoreactivity at 20 min, 120 min or 240 min of hyponatremia in the upper or deeper layers of the cerebellum, compared with the control animals, thus, it is unlikely that *de novo* protein synthesis could explain the observed short-term term differences. On the contrary, the immunoblot analysis revealed a significant decrease in the superficial parts of the neocortex at 4 h following induction of hyponatremia ($P < 0.05$).

A previous study showed a modestly increased AQP4 by immunoblot in whole brain and cerebellum in rat after 4 h after acute hyponatremia (Vajda et al., 2000). The discrepancy between the latter study and ours could be due to sampling (whole brain vs. cortical layers), species differences, or differences in the experimental protocols (2.5% Glucose solution vs. only water).

Proposed mechanism for short-term regulation

These early changes in immunolabelling after hyponatremia are likely to reflect either redistribution of AQP4 between membrane domains, vesicular intracellular transport or conformational changes altering the antigenicity.

The immunogold analysis showed a tendency, albeit modest, towards less labelling in the deeper layer of the cortex and the upper layers of the cerebellum.
However, the immunoblot analysis showed no changes in anti-AQP4 immunoreactivity between the superficial and deeper neocortical layers. Thus, a redistribution between layers is less likely. However, due to methodological constraints the dissected slices for immunoblot analysis were composed of several layers, thus limiting the comparability to the immunogold analysis.

The short-term regulation of AQP4 has been shown to be dependent on endocytotic pathways and the action of several kinases (Madrid et al., 2001; Carmosino et al., 2007). Thus, our results could plausibly be explained by decreased internalization of AQP4 or release from cytosolic vesicles. The dynamics of the AQP4 trafficking and recycling along the endocytic pathway *in vivo* is currently unknown

Hypertonic stress has been shown to increase the internalization of AQP4 in cell cultures (Madrid et al., 2001; Arima et al., 2003). On the other hand, hypoosmotic stress increases vesicle recycling in Intestine 407 cells (van der et al., 2003), but the effect of hypotonicity on endocytosis in glia and thus of AQP4 expression is currently not known. In *Xenopus laevis* oocytes activation of the $V1_aR$ with PKC dependent phosphorylation of serine 180 increased internalization of orthogonal arrays (OAPs) of AQP4 (Moeller et al., 2009). Thus, the expected decrease in AVP after induction of hyponatremia may dephosphorylate serine 180 and temporarily impede the internalization of AQP4.
Previous studies have indicated that brain could be under a tonic stimulation of AVP under physiological conditions (Niermann et al J. Neuroscience 2001)

The immunogold analysis revealed sparse intracellular labelling of AQP4
Thus, unlike the situation for AQP2 in the kidney, there is as yet no evidence for the existence of a significant vesicular pool of AQP4. Nevertheless, we cannot rule out that endosomal acidity and the adaptor proteins involved in clathrin-dependent endocytosis interacting with the C-terminus could shield the antigen from immunodetection. Recently, increasing data has elucidated the dynamics of OAP formation and disruption, where the M1/ M23 ratio regulates the size of the OAPs (Crane and Verkman, 2009; Crane et al., 2009a; Crane et al., 2009b). Consequently, the size of the OAPs could hypothetically alter the antigenicity through steric hindrance. Phosphorylation of residues in the C-terminus could also alter the conformation and immunolabelling of AQP4.

Finally, hypoosmotic stress has been shown to increase the extracellular concentration of glutamate, that may elicit Ca^{2+} wave propagation by activation of glial mGluRs.
Interestingly, a recent study has shown that glutamate induced calcium release may rapidly increase the water transport through AQP4 mediated by a CaMKII dependent phosphorylation of serine 111 (Gunnarson et al., 2008). Thus, glutamate is a prime candidate to be involved in regulation of AQP4 distribution and function in hyponatremia.

Proposed impact of rapid changes in AQP4 distribution on brain edema formation

Interestingly, those subpial membrane in the neocortex and granule cell layer in the cerebellar cortex that both displayed fast, dynamic changes are not dependent on α-syntrophin or dystrophin for the polarization of AQP4 (Amiry-Moghaddam et al., 2004b; Nicchia et al., 2008). Further, these membrane domains could be important efflux routes for bulk flow of water and osmolytes, when osmotic gradients force water into the brain. The surface area of the subpial membrane is significantly smaller than the total surface area of all the perivascular endfeet. Hence, regulation of water transport is probably even more important in the subpial membrane.

The observed differences in the short-term regulation of AQP4 could be a product of potential differences in the edema resolution between the neocortex and cerebellum.

The induction of hyponatremia will inevitably create a strong osmotic gradient that will force water into the brain. The main point is what implication this new finding might have in regard to the understanding of the directions of water after brain edema.

Several lines of evidence suggest that the initial, rapid response to acute hyponatremia is an increase in interstitial pressure, leading to shunting of fluid and solutes (i.e. Na^+ and Cl^-) from the interstitial space into the cerebrospinal fluid via the subpial membrane or ependyma and then into the systemic circulation (Melton et al., 1987). Hence, an ultra-fast upregulation of AQP4 in this domain in the neocortex would potentially increase the capacity for filtration of water and electrolytes (by increasing the permeability coefficient) through the subpial endfeet as a fast adapting, protective mechanism.

The brain also responds rapidly to hyponatremia by releasing K^+ and organic osmolytes (e.g taurine and myo-inositol) from neurons for subsequent uptake in adjacent glia (Lehmann et al., 1991). This mechanism only shifts volume from neurons to glia and represents no net change in brain water. Eventually, K^+ and the organic osmolytes are lost from the brain via perivascular glia. These changes will also contribute to reducing the osmotic gradient and impede the build-up of brain edema (Thurston et al., 1975; Sterns et al., 1993).

In conclusion, our data suggest that induction of hyponatremia elicits fast changes in AQP4 expression or conformation and that there are significant regional differences in response to

hyponatremia. These changes may reflect the observed differences in edema formation between brain regions.

Our main finding is that the subpial membrane undergoes a significant upregulation of AQP4 shortly after the onset of hyponatremia. A likely mechanism is that the decreased AVP will decrease the internalization of AQP4 and maybe also increase exocytosis.
Hence, this mechanism would make physiological sense as increased AQP4 may increase the efflux into the subarachnoid space that acts as a sink and decrease brain water content in hyponatremia (Hochwald et al., 1976).

Mouse model for bacterial meningitis

In order to further characterize the expression of AQP4 in CNS pathophysiology and the impact of AQP4 in brain edema formation we established a mouse model for bacterial meningitis in paper IV. In the presented model, *N. meningitidis* was infused into the CSF through an incision in the skull near the bregma. Addition of iron to the infusate selectively enhanced the development of meningitis rather than sepsis.

As *N. meningitidis* is not normally a pathogen in mice, the extrapolation from experimentally induced meningitis in mice to clinical meningitis in man is a daunting task.
However, the mice showed a plethora of signs consistent with clinical meningitis.
The immune system was activated as expression of *Tnf-α*, a marker for severe inflammation, was increased severalfold. Further, streaking of CSF samples produced colonies of Mc on blood agars. The mice showed fever, reduced locomotion, fatigue and weight loss; all clinical signs of meningitis.

The *Tnf-α* gene expression was increased in mice infected with Mc after 9 hours, but only in the core brain. However, after 30 h the inflammation was mostly confined to the brain surface. One explanation for this counterintuitive finding is that shortly after Mc infection there is no predominant meningitis, but a general, global inflammatory response. The pathoanatomic analysis did not reveal visible inflammation in the brain or meninges after only 9 h. The *Tnf-α* upregulation could be mainly due to blood in the brain, thus not really a cerebral inflammation.

However, after 30 h almost every animal with MC show meningeal inflammation as a sign of meningitis. Consequently, *Tnf-α* is also increased at the brain surface.

As the bacteria were directly inoculated into the CSF, this model does not enable the investigation of the crucial pathophysiological steps from a commensal microbe in the upper airways and the subsequent interaction with the blood-brain barrier and the penetration into the brain, yielding meningitis. This notwithstanding, we believed that the model could be an excellent tool for exploring the host-pathogen interaction of a specific number of defined bacteria after penetration into the brain.

Impact of AQP4 gene deletion on brain edema formation in meningococcal meningitis

In paper V we utilized the model presented in paper IV to study the impact of infection with *N. meningitidis* on AQP4 expression and brain water dynamics in wild type mice and AQP4 null mice. Currently, there seems to be uncertainty as to the prevalence and mechanism of brain edema in meningococcal meningitis. Diffusion-weighted MRI data suggest that the early edema formation in meningococcal meningitis is primarily cortical and cytotoxic (Citton et al., 2009).

Interestingly, the degree of concomitant bacteremia seems to modulate the formation of brain edema, at least in pneumococcal meningitis (Brandt et al., 2008). Loss of cerebral autoregulation is also common in acute bacterial meningitis: Increasing the ICP and the hydrostatic driving force for water into the CNS (Pedersen et al., 2007).
Acute inflammation of the meninges is also likely to increase the resistance of cerebral fluid outflow through the subpial membrane and ependymal lining and a degree of hydrocephalic edema is expected. In these circumstances, AQP4 could be critically involved in the resolution of the edema by facilitating bulk flow through these natural efflux routes.

The facts that we observed an increase in brain water in AQP4 KO after induction of meningococcal meningitis, and that the blood-brain barrier seemed to be intact in the mouse meningitis model, are not consistent with an early cytotoxic edema only, but more in line with a component of hydrocephalic edema.

Unexpectedly, we found no evidence for up-regulation of AQP4 in pneumococcal or meningoccal meningitis. Moreover, a quantitative immunoblot revealed a significant decrease

in AQP4 immunolabelling in mice infected with *S. pneumoniae* for 30 h. These findings are in clear contrast to the reported severalfold increase in AQP4 expression after pneumoccal meningitis (Papadoupoulos and Verkman, 2005). Moreover, in another study, intracerebrospinal administration of IL-1β led to a significant upregulation of AQP4 (Ito et al., 2006). Interestingly, inhibition of the nuclear factor-κB pathway abolished the induction of AQP4. Our finding that the gene expression of AQP4 was increased 4-fold in mice injected with lipo-oligosaccharide (LOS) for 9 and 30 h in the core brain, but not in the brain surface, is intriguing. Hence, it could be that astrocytes near the brain surface respond differently to LOS than astrocytes in the core brain.

In the previous study (Papadopoulos and Verkman, 2005), also a model with direct inoculation, the design was much rougher with the needle penetrating the parenchyma before depositing the bacteria into the basal cisterna. This is likely to cause tissue damage and bleeding which could hypothetically in combination with *S. pneumoniae* alter AQP4 expression. One must also keep in mind that the cell wall components of *S. pneumoniae* and *N. meningitidis* (peptidoglycan and LOS, respectively) activate partly different cascade systems, in addition to the common effects through IL-1.

Vasopressin is often significantly elevated in bacterial meningitis (Leclerc et al., 2003). There is experimental evidence that elevated vasopressin, activating its receptor ($V1_aR$), and phosphorylation of serine 180 by PKC, increases internalization of OAPs (Moeller et al., 2009). Nevertheless, the precise mechanisms for regulation of AQP4 in meningitis are still obscure and warrant further studies.

Overall conclusion

The present study has shown that AQP4 expression is dynamic and that the response of AQP4 to experimental insults or disease differs between brain regions and membrane domains (cf. hypothesis), probably as a consequence of different anchoring mechanisms (cf. hypothesis).

8.2 Methodological considerations

The overriding goal of this thesis was to explore the expression and polarization of AQP4 during pathogenesis. AQP4 can be visualized by several methods, but only electron microscopy has good enough resolution to show that AQP4 is selectively polarized in astrocytic endfeet and not in the adjacent epithelial membrane (Nielsen et al., 1997).

Postembedding electron microscopy

The hallmark of postembedding immunocytochemistry is that the tissue is embedded in a resin prior to the immunocytochemical procedure followed by an electron microscopic analysis. The ultimate goal in postembedding immunocytochemistry is to achieve a representative ultrastructure of the tissue combined with efficient labeling of the proteins of interest. In practice, the first desire conflicts with the latter.

The resolution of the postembedding method is restricted only by the length of the antibody bridge and the diameter of the gold particle. In theory, the distance between the gold particle and the epitope should correspond to the radius of the gold particle plus the length of the interposed immunoglobulins. Using 15 nm gold particles and a primary and secondary IgG (each with a length of 8 nm) this distance should be roughly 23 nm.

To obtain excellent specificity it is very important to keep background labeling at a minimum. Since immunoreagents tend to show low-affinity, unspecific binding to tissue proteins it is important to add some proteins to the buffer solutions to block this binding.
Usually, with 2% HSA included in the solution we obtain very low background labeling combined with a strong specific signal.

The postembedding technique only allows immunodetection of those antigens that are exposed at the surface of the section. This implies that the proportion of antigen available for immunodetection is severely restricted compared to other immunocytochemical approaches. Many parameters in the incubation protocol may affect the strength of the immunogold signal. On a general basis, the signal is strengthened with increased concentration of the primary antibody and reduced concentration of saline. However, with high antibody concentrations there is also a risk for increased unspecific binding. Careful experimentation is required to identify the conditions that give the highest signal-to-noise ratio for a given antibody.

When the labeling efficiency and specificity are high the postembedding method is semiquantitative and a near linear correlation exists between antigen concentration and immunosignal (Ottersen, 1989). Luckily, we have thus far been granted with very good commercial anti-AQP4 antibodies, yielding strong labeling (sensitivity) with minimal background labeling,

Sampling of the material for the electron microscopic analysis

In all the capturing of the electron microscopic pictures the investigator has been blinded to the tissue on the examined grids. In our lab, the technicians at the lab reorder the grids by a written code in the grid box unaware of the tissue on the grids. The images are also analyzed blinded to the investigator. Thus, because the investigator is unaware of exactly the grids this should rule out a lot of the potential bias.

In paper II and paper III we have discriminated between different regions and layers in our analyses. In paper I the sampling in retina did not discriminate between the different layers and regions (central/ peripheral) or between the different glial cells (Müller cells vs. astrocytes). As retina consists of several different layers, we can not rule out regional differences in the retina.

Image capturing and image analysis

In the subsequent electron microscopic analysis it is important to choose an electron optic magnification that represents a good compromise between digital resolution, required field of view and the size of the digital image file.

Our main tool for quantifying immunogold labeling is ANALYSIS, created in our laboratory (Haug et al., 1994; Haug et al., 1996) in collaboration with Soft Imaging Systems Gmbh in Germany as an extension to their commercial software.

In brief, transected organelles are drawn freehand as regions of interest (ROIs) and membranes as curves. As already discussed the theoretical distance between the antigen of interest and gold particle is approx. 23 nm. We usually sample gold particles within 30 nm of either side of the membrane. Particles further away from the membrane are eliminated. Gold particles along a curve (i.e. membrane) are measured as linear densities, while gold particles in a ROI are measured as areal densities. For instance, in the analysis of perivascular AQP4

expression, the ROI is the “perivascular endfeet” and the curve of interest is the “perivascular membrane”.

Although the calculation of gold particles is done automatically, it is necessary to carefully inspect the results and optimize the parameters, if required. In some cases one has to interactively delete, add, or split particles. Thus the quality of the quantitative analysis depends on the skills of the operator. In ANALYSIS, an image with associated ROIs, curves, and particles is termed a field. Finally, linear density of particles per curve and areal density of particles per ROI are aggregated over the project and exported to SPSS, and the fields are subjected to statistical analysis.

Freeze-fracture electron microscopy

In brief, in the freeze-fracturing method the specimen is fixed in formaldehyde, frozen in liquid nitrogen, and then fractured by a knife in vacuum. Carbon-platinum replicas of the fracture faces are made by shadowing the surface at narrow angles and then digesting away the tissue. When the replicas are examined in the electron microscope, it is seen that cell membranes caught in the cleavage plane are split down the middle of their lipid layer where the molecular binding is weakest. This exposes one of two complementary faces: the P face, which represents the external aspect of the inner cytoplasmic leaflet, and the E face, which represents the internal aspect of the outer cytoplasmic leaflet. The true inner and outer surfaces of the plasma membrane are not exposed by this method.

In mammals, proteins generally adhere to the P face, whereas “pits” in the E face represent imprints of the membrane protein. The assemblies of proteins seen in the P- and E- face are called intramembrane particles (IMPs).

Interestingly, early freeze fracture studies revealed abundant “square arrays” of IMPs in freeze-fractured membranes of astrocytes, called OAP (orthogonal array of particles) (Dermietzel, 1974). AQP4 KO mice lacked OAPs in the plasma membrane of astrocyte endfeet and in other AQP4 expressing tissues and we now know that OAPs is in fact orthogonal arrays of AQP4 tetramers (Verbavatz et al., 1997; Rash et al., 1998).

Real-time PCR of Aqp4 and Tnf-α

The procedure follows the general priniciple of a polymerase chain reaction, but the key feature is that RNA is isolated, converted to cDNA and the amplified cDNA is detected in real time as the reaction progresses.

This unique advantage makes the method quantitative. The amplified DNA may detected by a non-specific fluorescent dye intercalating with DNA or sequence-specific DNA probes that are labelled with a fluorescent reporter. We have utilized the non-specific SYBR Green dye. However, this dye will bind to all dsDNA PCR products, such as primer dimer, and this can potentially prevent accurate quantification of the intended target sequence.

The values obtained by the PCR instrument have no absolute unite, but can only give a fraction or ratio relative to a standard.

Further, the relative concentrations of DNA during the exponential phase of the reaction are plotted against a logarithmic scale. The cycle where the fluorescence crosses this straight line, is called the cycle threshold (Ct). Thus, a sample whose Ct is 4 cycles earlier than another's has $2^4 = 16$ times more template.

In paper IV and paper V, PCR was performed in four parallel reactions for each gene studied, per animal studied. The purity of the amplified product was confirmed with the dissociation curve and gel electrophoresis of selected samples. Relative quantitation was achieved by using the comparative C_T method. In order to correct for differences in the amount and quality of cDNA added to the reaction, the housekeeping gene *Gapdh* was used as an endogenous reference, and the results for *Aqp4* and *Tnf-α* were normalized to those from *Gapdh* PCR in individual samples. Results were then normalized to a calibrator sample, and the relative expression was obtained, providing indirect information on target mRNA levels.

Immunoblotting of AQP4

Good resolution could also be a disadvantage: It is difficult to quantify the total levels of AQP4 in brain, irrespective of glial domains. In hyponatremia and meningitis we were interested in the total amount of AQP4 in brain. Thus, here the method of choice is SDS-PAGE (paper III and paper V). Proteins can here be measured by quantifying the density of the protein bands on a blot. However, the method has great internal variability and the result from one experiment is often difficult to replicate. But with care and concern of the most common pitfalls the reproducibility will eventually be satisfying.

1) The amount of protein loaded should be in the linear range of the standard curve.
It is of utmost importance that the protein concentrations in samples are accurately measured so that the total protein loaded in each lane is equal. First the protein concentrations in the samples are measured in triplicate with a spectrophotometer. The separation of proteins on the gel is primarily dependent on their molecular weights. The difference in molecular weight of the two isoforms of AQP4 is only 2 kDa and to increase the resolution 9 M urea was added to the gels.

2) The transfer from gel to membrane has high variability between gels, but also on the same gel, the transfer may be unequal. Thus, it is of paramount importance to repeat the experiments.

3) The incubation of the membrane in primary and secondary antibodies is a critical step.
The antibody concentration should ideally be titrated on a dot plot membranes.
However, it is of crucial importance that the membranes are blocked with milk powder before incubation with antibodies.

4) The membranes are incubated in secondary alkaline phosphate-linked immunoglobulin, followed by addition of ECF substrate. The alkaline phosphatase catalyzes the conversion of ECF substrate to a highly fluorescent product which fluoresces strongly at 540-560 nm. The strength of the individual bands may be analyzed and quanitied with commercial available image programmes (e.g. Image Quant, GE Health). The strength of the ECF reaction has a linear correlation with the amount of proteins in the samples as long as the signal is not oversaturated.

5) After the first incubation with anti-AQP4 antibodies and subsequent analysis it is paramount to reprobe with antibodies against a structural housekeeping gene, such as β-actin, to adjust for unequal protein loading.

Brain water measurement
In paper V we wanted to get an objective measurement of brain edema formation. To measure brain water we employed the wet/dry-methodology. Thus, the brain is weighed in a pre-weighed glass beaker on an analytical balance, dried for 24 h at 80°C in a vacuum oven. The

dried tissue is reweighed and the total brain water may be computed by the equation (wet brain (mg) – dry brain (mg)/ wet brain mg). The method has several pitfalls. It is of outmost importance that the brains are removed and homogenized in the same way. An 80°C 10 gram glass beaker will have a slight decrease in mass, but this can give an inaccuracy of 2-3% on the brain water measurements. Thus, the glass beaker should cool to room temperature.

Middle cerebral artery occlusion (MCAO)

In paper II we aimed at exploring the expression of AQP4 after ischemia. We chose to use a validated mouse model. MCAO is a stroke model in rodents and mimics the effects of a stroke in human. In brief, the skin was opened with a midline incision and the underlying submandibular gland and omohyoid muscle where dissected to reveal the common carotid artery. Then, the external carotid artery was ligated distally and divided. Next, aneurysm clips was applied to the internal carotid artery and common carotid artery. Finally, a 5-0 nylon filament was advanced through the external carotid artery stump through a point 6 mm distal to the carotid bifurcation. The occlusion of the middle cerebral artery was verified at 30 min by allowing the animal to awaken and performing neurological deficit scoring as follows: 0, normal motor function; 1, flexion of torso and of contralateral forelimb upon lifting by the tail; 2, circling to the contralateral side but normal posture at rest; 3, leaning to the contralateral side at rest; 4, no spontaneous motor activity. Mice with clear neurological deficits (score of ≥ 2) were reanesthetized for withdrawal of the suture and reperfusion after 90 min of MCAO.

50% of all stroke cases are due to an occlusion of the middle cerebral artery. So far, it has been difficult to construct good models for human stroke. This could be due to the complexity and size of the human brain or, maybe even more importantly, that humans and rodents differ in regard to the vascularization and composition of the brain parenchyma. Further, in humans white matter constitutes ~40% of the brain, compared to ~10% in rodents. Stroke in humans predominantly involve white matter, whereas rodent models primarily assess grey matter damage. Thus, this represents an intrinsic bias in all currently available rodent models. This notwithstanding, MCAO has proved valuable as a model for recanalized stroke in humans.

Mouse model for acute hyponatemia

In paper III we utilized a mouse model for acute induction of hypotonic hyponatremia "water intoxication". In this model the mice receive a 10% of body weight bolus of ion free water with a vasopressin receptor II antagonist (0.4 μg/kg) intraperitoneal. The dilutional effect of the added water will inevitably yield hyponatremia. The pro of this model is that it is fast and easily reproducible model, with no major confounding factors. However, the pathophysiological relevance to hyponatremia in human may be debated. In man, hyponatremia is often caused by an underlying, pathogenic process.

This notwithstanding, severe hyponatremia may already develop during a 2 ½ h Marathon race in healthy athletes (Almond et al., 2005). Excess intake of fluids, extensive sweating and reduced kidney function (sympaticus activity during the race and painkillers (NSAIDs)) all contribute in lower serum sodium. Thus, the slope of the drop of serum sodium may be similar to the acute mouse model, but this is currently unknown as blood samples are only taken after the race. In effect, we believe that the model is a valid model for acute hypotonic, dilutional hyponatremia.

Models for experimental meningitis

Backdrop

The recent development of murine models for bacterial meningitis offers tools for exploring the host-pathogen interaction *in vivo* (Chiavolini et al., 2008).

Two major types of murine meningitis models exist: 1) direct infection by the intracerebral or the intracisternal route or 2) infection induced by the intraperitoneal or intranasal route. Direct bacterial inoculation into the CNS mimics the contiguous spread of bacteria from the nasopharynx or traumatic inoculation into the brain.

Thus, this allows the study of host-pathogen interactions once infection is established in the meninges, but does not enable the analysis of the different pathogenic steps occurring from colonization to disease in the CNS. In contrast, meningitis induced via intranasal or intraperitoneal routes is useful for the analysis of the pathogenesis according to the natural way of infection, but the model is hampered by the fact that many mice die of disseminated sepsis without ever developing meningitis.

As *S. pneumonia* is a naturally virulent pathogen in mice, the current models are only validated with pneumococcal meningitis (Chiavolini et al., 2004; Orihuela et al., 2009). Alas, since *N. meningitidis* is a human-specific pathogen there have thus far not been any good animal models for meningococcal meningitis available (Johansson et al., 2005; Zarantonelli et al., 2007).

In order to benefit from the ever increasing number of transgenic mice strains it is paramount to establish a valid mouse model for meningococcal meningitis.

Method

We utilized the direct inoculation approach, with modified protocol from Chiavolini *et al*., 2004. Meningitis was introduced in mice by intracranial *(i.c.)* injection of live meningococci. Mice were anesthetized with a subcutaneous injection (*s.c*.) of fentanyl/fluanison and benzodiazepine (Hypnorm/Dormicum) and the head was secured in a stereotactic frame. The skin on top of the head was incised and the bregma was then localized, and a burr hole was made 0 mm lateral and 3.5 mm rostral to the bregma. A blunted 30-gauge needle attached to a gas-tight glass syringe was stereotactically introduced through the burr hole, 2 mm ventral. After 1 min, the challenge dose was infused using an injection pump set at 5 µl/min, and 30 sec after complete injection, the needle was gradually removed. In control studies only saline and Fe was infused. The whole in the scalp and the skin opening on top of the head were closed using bonewax and topical tissue adhesive, respectively. Intra peritoneal (*i.p*.) injections of Fe were given to selected mice to enhance the Mc infection. Pain relief (Temgesic) or eye protection was administered. Mice were either wrapped in paper to keep warm (i.e. no specific temperature control) or the body temperature was regulated using a heating lamp. Temperature controlled animals received subcutaneous injections of 0,5 ml 0,85% saline at 0, 5 and 20 h post injection and rectal temperature was monitored at the same intervals.

The mice were humanly sacrificed by decapitation or cardiac puncture at different time intervals post infection. In cases of severe symptoms, the mice were humanly sacrificed immediately. After sacrifice, CSF and blood samples were collected and inoculated on 5% human blood agar. Mice brains were surgically removed and processed for further analyses.

8.3 Future perspectives

The present thesis work has addressed central issues in brain pathophysiology. A number of questions will have to be addressed in future studies: What is the physiological importance of OAPs formation, and how is single channel AQP4 water permeability regulated?
Does AQP4 modulate the function of other molecules (e.g. ion channels), facilitate the movement of solutes or contribute in osmosensing?
What are the direction and magnitude of water transport through AQP4 in different membrane domains in physiology and during pathogenesis?

I shall limit myself to elaborate on the more concrete approaches that could be derived from this thesis.

Our finding in paper I warrant further studies aiming at unraveling the mechanism for the proposed α-syntrophin independent pool of AQP4 in the retina, where other syntrophin members (e.g. β_1-syntrophin) are prime candidates as well as members of the utrophin complex. It is also important to resolve the molecular basis for anchoring of AQP4 in the subpial membrane and other dystrophin independent domains in the brain and the mechanisms for local regulation of AQP4 in the brain. Further, it is of utmost importance to unravel the hitherto unknown protein that is responsible for the anchoring of AQP4 in concert with Dp71 and α-syntrophin in the brain and retina.

Our main finding in paper II that AQP4 undergoes a dramatic downregulation in the infarction core warrants further insight into the potential mechanisms involved. In ischemia and reperfusion the cells undergo dramatic metabolic and molecular changes and thus a plethora of mechanism could be involved. However, one prime candidate is the MMPs that have been shown to be consistently involved in blood-brain barrier distruption, subsequently leading to vasogenic edema. The DAPC is attached through dystroglycans to laminin and agrin, both substrates for MMPs. Therefore, *in vitro* single molecular tracking of AQP4 after activation of MMPs could elucidate the impact of proteolysis on AQP4 expression.
AVP is often non-specifically released in acute intracranial pathology.
There is substantial evidence that activation of the V_1-receptor and PKC, may phosporylate and downregulate AQP4. A phosphorylation assay after MCAO could elucidate if AQP4 is massively phosphorylated in stroke.

In paper III, our finding that AQP4 undergoes dynamic changes in the subpial and other membranes after hyponatremia, whereas the total protein expression is unchanged in immunoblot analysis, begs the question if the OAPs structure and immunoreactivity is changed. One feasible approach is to assess the OAPs with freeze fracture. Further, to unravel the phosphorylation dynamics a phosphorylation assay is of paramount importance. A possible experiment to elucidate the importance of the subpial pool in the clearance of water during hyponatremia by bulk flow into the SAS would be to administer AQP4 inhibitors into the CSF that could selectively block the pool of APQ4 in the subpial membrane.

As the predominant type (if any in particular) of edema in meningitis is still not clear-cut a DWI MRI is a natural step forward to gain understanding of the edema mechanisms in our new mouse model for meningococcal meningitis, as the diffusion is increased in vasogenic and hydrocephalic edema, but decreased in cytotoxic brain swelling.

AQP4 as a therapeutic target

AQP4 is undoubtedly a promising target for therapeutic intervention both in stroke, hyponatremia and meningitis as discussed in this thesis.
Thus far, we do not have an adequate molecular understanding of how we should target AQP4. We need more basic understanding of AQP4 in normal brain physiology before we can consider manipulating AQP4.

We must not forget that the complexity of the human blood-brain barrier impedes the access of drug candidates to their intracerebral targets. Nevertheless, the current construction of small molecular ligands will be an important step in validating the therapeutic potential of AQP4 inhibition. One possible approach is to construct peptides with high affinity to PDZ domains that could compete with the binding between the terminal SSV sequence of AQP4 and its anchoring molecule, α-syntrophin.

Peptide ligands are likely to be inefficient as the BBB has low permeability to peptides. But, peptides could be conjugated to more lipophilic substances or could be used as 3D models for the generation of non-peptide ligands. The timing for application of potential AQP4 inhibitors is of utmost importance, given the specific time course of changes observed after MCAO (present study). Clearly, more work needs to be done in order to provide a platform for a novel therapy for brain edema.

The polarization of AQP4 in the perivascular endfeet is contingent on OAPs.
Hitherto, the exact role of OAPs formation in controlling single channel water transport is unresolved. Palmitoylation has been shown to regulate the size, an maybe the water transport, through OAPs. Thus, AQP4 could potentially be targeted by manipulating the formation of OAPs.

A future therapy based on AQP4 inhibition can be expected to offer only partial protection against edema formation. Water may diffuse through the narrow slits that separate the endfeet and might also be transported along with other molecules. It should also be recalled that water is able to diffuse (albeit at a very low rate) through the lipid bilayer of the plasma membrane. Besides, in the vasogenic phase of a postischemic edema, the blood-brain barrier breaks down, leading to extravasation of albumin and other plasma proteins. Hence, osmotic forces and the loss of blood-brain barrier integrity will lead to influx of water independently of AQP4. But AQP4 could be of benefit by stimulating bulk flow of water and osmolytes out of the brain as to counteract the edema formation.

It should be emphasized that there are several other potential therapeutic targets in early brain edema formation. Proposed key players are cotransporters such as NKCC1, where the loop diuretic bumetanide is a promising candidate. In fact, there is recent evidence that bumetanide may inhibit AQP4 water permeability in *Xenopus* oocytes and downregulate perivascular AQP4 during transient ischemia (Migliati et al., 2009; Migliati et al., 2010). If so, the use of a previously approved drug may by pass many hurdles for AQP4 as a target in protection against brain edema. An approach directing both cotransporters and AQP4 are likely to be efficient in reducing edema formation.

Further, glutamate excitotoxicity, caused by excessive glutamate release during an ischemic event, is a major contributing factor to neuronal perturbation and subsequent apoptosis. In stroke, glutamate excitotoxicity and edema formation mutually aggravate each other. Future therapy should target both glutamate excitotoxicity and edema formation to interrupt this vicious circle. Such a combined approach, targeting several molecular pathways, would hopefully have an additive effect on reducing the edema formation and improve the prognosis of cerebral brain edema.

9. CONCLUDING REMARKS

Brain edema is still in the 21st century a feared complication in a plethora of intracranial and systemic disorders. AQP4 is a promising target for therapeutic intervention targeting brain edema. However, AQP4 has shown to be a Janus-faced player in brain edema formation as AQP4 has a deleterious effect in mouse models with cytotoxic and osmotic brain edema, whereas AQP4 has a protective role in models of vasogenic and hydrocephalic edema.

This thesis has further explored the expression and polarization of AQP4 in relevant pathologies. Thus, it is of paramount importance to know the spatiotemporal changes of AQP4 expression in the disease process. The main conclusion is that AQP4 undergoes dynamic changes both in polarization and distribution. This new knowledge should be emphasized in the consideration of AQP4 as a therapeutic target

10. REFERENCE LIST

Reference List

Adams ME, Butler MH, Dwyer TM, Peters MF, Murnane AA, Froehner SC (Two forms of mouse syntrophin, a 58 kd dystrophin-associated protein, differ in primary structure and tissue distribution. Neuron 11:531-540.1993).

Adams ME, Kramarcy N, Krall SP, Rossi SG, Rotundo RL, Sealock R, Froehner SC (Absence of alpha-syntrophin leads to structurally aberrant neuromuscular synapses deficient in utrophin. J Cell Biol 150:1385-1398.2000).

Adams ME, Mueller HA, Froehner SC (In vivo requirement of the alpha-syntrophin PDZ domain for the sarcolemmal localization of nNOS and aquaporin-4. J Cell Biol 155:113-122.2001).

Adrogue HJ, Madias NE (Hyponatremia. N Engl J Med 342:1581-1589.2000).

Agre P, King LS, Yasui M, Guggino WB, Ottersen OP, Fujiyoshi Y, Engel A, Nielsen S (Aquaporin water channels--from atomic structure to clinical medicine. J Physiol 542:3-16.2002).

Almond CS, Shin AY, Fortescue EB, Mannix RC, Wypij D, Binstadt BA, Duncan CN, Olson DP, Salerno AE, Newburger JW, Greenes DS (Hyponatremia among runners in the Boston Marathon. N Engl J Med 352:1550-1556.2005).

Amiry-Moghaddam M, Frydenlund DS, Ottersen OP (Anchoring of aquaporin-4 in brain: molecular mechanisms and implications for the physiology and pathophysiology of water transport. Neuroscience 129:999-1010.2004a).

Amiry-Moghaddam M, Otsuka T, Hurn PD, Traystman RJ, Haug FM, Froehner SC, Adams ME, Neely JD, Agre P, Ottersen OP, Bhardwaj A (An alpha-syntrophin-dependent pool of AQP4 in astroglial end-feet confers bidirectional water flow between blood and brain. Proc Natl Acad Sci U S A 100:2106-2111.2003a).

Amiry-Moghaddam M, Williamson A, Palomba M, Eid T, de Lanerolle NC, Nagelhus EA, Adams ME, Froehner SC, Agre P, Ottersen OP (Delayed K+ clearance associated with aquaporin-4 mislocalization: phenotypic defects in brains of alpha-syntrophin-null mice. Proc Natl Acad Sci U S A 100:13615-13620.2003b).

Amiry-Moghaddam M, Xue R, Haug FM, Neely JD, Bhardwaj A, Agre P, Adams ME, Froehner SC, Mori S, Ottersen OP (Alpha-syntrophin deletion removes the perivascular but not endothelial pool of aquaporin-4 at the blood-brain barrier and delays the development of brain edema in an experimental model of acute hyponatremia. FASEB J 18:542-544.2004b).

Arima H, Yamamoto N, Sobue K, Umenishi F, Tada T, Katsuya H, Asai K (Hyperosmolar mannitol simulates expression of aquaporins 4 and 9 through a p38 mitogen-activated protein kinase-dependent pathway in rat astrocytes. J Biol Chem 278:44525-44534.2003).

Auguste KI, Jin S, Uchida K, Yan D, Manley GT, Papadopoulos MC, Verkman AS (Greatly impaired migration of implanted aquaporin-4-deficient astroglial cells in mouse brain toward a site of injury. FASEB J 21:108-116.2007).

Avery OT, Dubos R (THE PROTECTIVE ACTION OF A SPECIFIC ENZYME AGAINST TYPE III PNEUMOCOCCUS INFECTION IN MICE. J Exp Med 54:73-89.1931).

Bauserman SC, Naul GL (2003) The neuropathology in Mc pathology is characterized by edema. In: Bacterial, fungal and parasitic diseases of the central nervous system. In: Nelson, J.S; Mena H; Parisi, J.E and Schochet Jr, S.S. Principles amd Practice of Neuropathology, vol. 2nd ed., pp 45-77.

Bereczki D, Fekete I, Prado GF, Liu M (Mannitol for acute stroke. Cochrane Database Syst Rev:CD001153.2007).

Bereczki D, Liu M, do Prado GF, Fekete I (Mannitol for acute stroke. Cochrane Database Syst Rev:CD001153.2001).

Binder DK, Oshio K, Ma T, Verkman AS, Manley GT (Increased seizure threshold in mice lacking aquaporin-4 water channels. Neuroreport 15:259-262.2004a).

Binder DK, Papadopoulos MC, Haggie PM, Verkman AS (In vivo measurement of brain extracellular space diffusion by cortical surface photobleaching. J Neurosci 24:8049-8056.2004b).

Bloch O, Auguste KI, Manley GT, Verkman AS (Accelerated progression of kaolin-induced hydrocephalus in aquaporin-4-deficient mice. J Cereb Blood Flow Metab 26:1527-1537.2006).

Bloch O, Papadopoulos MC, Manley GT, Verkman AS (Aquaporin-4 gene deletion in mice increases focal edema associated with staphylococcal brain abscess. J Neurochem 95:254-262.2005).

Bordey A, Spencer DD (Distinct electrophysiological alterations in dentate gyrus versus CA1 glial cells from epileptic humans with temporal lobe sclerosis. Epilepsy Res 59:107-122.2004).

Brandt CT, Holm D, Liptrot M, Ostergaard C, Lundgren JD, Frimodt-Moller N, Skovsted IC, Rowland IJ (Impact of bacteremia on the pathogenesis of experimental pneumococcal meningitis. J Infect Dis 197:235-244.2008).

Bulfield G, Siller WG, Wight PA, Moore KJ (X chromosome-linked muscular dystrophy (mdx) in the mouse. Proc Natl Acad Sci U S A 81:1189-1192.1984).

Carmosino M, Procino G, Tamma G, Mannucci R, Svelto M, Valenti G (Trafficking and phosphorylation dynamics of AQP4 in histamine-treated human gastric cells. Biol Cell 99:25-36.2007).

Chang CJ, Chang WN, Huang LT, Huang SC, Chang YC, Hung PL, Lu CH, Chang CS, Cheng BC, Lee PY, Wang KW, Chang HW (Bacterial meningitis in infants: the epidemiology, clinical features, and prognostic factors. Brain Dev 26:168-175.2004).

Chiavolini D, Pozzi G, Ricci S (Animal models of Streptococcus pneumoniae disease. Clin Microbiol Rev 21:666-685.2008).

Chiavolini D, Tripodi S, Parigi R, Oggioni MR, Blasi E, Cintorino M, Pozzi G, Ricci S (Method for inducing experimental pneumococcal meningitis in outbred mice. BMC Microbiol 4:36.2004).

Citton V, Toldo I, Calderone M, Sartori S, Manara R (Early cortical cytotoxic edema in meningococcal meningitis. Pediatr Neurol 41:146-150.2009).

Crane JM, Bennett JL, Verkman AS (Live cell analysis of aquaporin-4 m1/m23 interactions and regulated orthogonal array assembly in glial cells. J Biol Chem 284:35850-35860.2009a).

Crane JM, Tajima M, Verkman AS (Live-cell imaging of aquaporin-4 diffusion and interactions in orthogonal arrays of particles. Neuroscience.2009b).

Crane JM, Verkman AS (Determinants of aquaporin-4 assembly in orthogonal arrays revealed by live-cell single-molecule fluorescence imaging. J Cell Sci 122:813-821.2009).

Dalloz C, Sarig R, Fort P, Yaffe D, Bordais A, Pannicke T, Grosche J, Mornet D, Reichenbach A, Sahel J, Nudel U, Rendon A (Targeted inactivation of dystrophin gene product Dp71: phenotypic impact in mouse retina. Hum Mol Genet 12:1543-1554.2003).

Davidsen T, Koomey M, Tonjum T (Microbial genome dynamics in CNS pathogenesis. Neuroscience 145:1375-1387.2007).

Davidsen T, Tonjum T (Meningococcal genome dynamics. Nat Rev Microbiol 4:11-22.2006).

de Groot BL, Engel A, Grubmuller H (A refined structure of human aquaporin-1. FEBS Lett 504:206-211.2001).

de Groot BL, Grubmuller H (Water permeation across biological membranes: mechanism and dynamics of aquaporin-1 and GlpF. Science 294:2353-2357.2001).

Dermietzel R (Junctions in the central nervous system of the cat. 3. Gap junctions and membrane-associated orthogonal particle complexes (MOPC) in astrocytic membranes. Cell Tissue Res 149:121-135.1974).

Dietzel I, Heinemann U, Hofmeier G, Lux HD (Stimulus-induced changes in extracellular Na+ and Cl- concentration in relation to changes in the size of the extracellular space. Exp Brain Res 46:73-84.1982).

Edmond K, Clark A, Korczak VS, Sanderson C, Griffiths UK, Rudan I (Global and regional risk of disabling sequelae from bacterial meningitis: a systematic review and meta-analysis. Lancet Infect Dis 10:317-328.2010).

Eid T, Lee TS, Thomas MJ, miry-Moghaddam M, Bjornsen LP, Spencer DD, Agre P, Ottersen OP, de Lanerolle NC (Loss of perivascular aquaporin 4 may underlie deficient water and K+ homeostasis in the human epileptogenic hippocampus. Proc Natl Acad Sci U S A 102:1193-1198.2005).

Fenton RA, Moeller HB, Zelenina M, Snaebjornsson MT, Holen T, Macaulay N (Differential water permeability and regulation of three aquaporin 4 isoforms. Cell Mol Life Sci 67:829-840.2010).

Fort PE, Sene A, Pannicke T, Roux MJ, Forster V, Mornet D, Nudel U, Yaffe D, Reichenbach A, Sahel JA, Rendon A (Kir4.1 and AQP4 associate with Dp71- and utrophin-DAPs complexes in specific and defined microdomains of Muller retinal glial cell membrane. Glia 56:597-610.2008).

Fushimi K, Uchida S, Hara Y, Hirata Y, Marumo F, Sasaki S (Cloning and expression of apical membrane water channel of rat kidney collecting tubule. Nature 361:549-552.1993).

Galloway WA, Murphy G, Sandy JD, Gavrilovic J, Cawston TE, Reynolds JJ (Purification and characterization of a rabbit bone metalloproteinase that degrades proteoglycan and other connective-tissue components. Biochem J 209:741-752.1983).

Goldschneider I, Gotschlich EC, Artenstein MS (Human immunity to the meningococcus. I. The role of humoral antibodies. J Exp Med 129:1307-1326.1969a).

Goldschneider I, Gotschlich EC, Artenstein MS (Human immunity to the meningococcus. II. Development of natural immunity. J Exp Med 129:1327-1348.1969b).

Gorelick DA, Praetorius J, Tsunenari T, Nielsen S, Agre P (Aquaporin-11: a channel protein lacking apparent transport function expressed in brain. BMC Biochem 7:14.2006).

Gunnarson E, Zelenina M, Axehult G, Song Y, Bondar A, Krieger P, Brismar H, Zelenin S, Aperia A (Identification of a molecular target for glutamate regulation of astrocyte water permeability. Glia.2008).

Hanna FW, Scanlon MF (Hyponatraemia, hypothyroidism, and role of arginine-vasopressin. Lancet 350:755-756.1997).

Haug FM, Desai V, Nergaard PO, Laake JH, Ottersen OP. Particle- counting in immunogold labelled ultrathin sections by transmission electron microscopy and image analysis. [Anal. Cell. Pathol]. 1994.
Ref Type: Generic

Haug FM, Desai V, Nergaard PO, Ottersen OP. Quantifying immunogold labelled receptors and transmitter by image analysis. [Soc. Neurosci. Abstr.]. 1996.
Ref Type: Generic

Hochwald GM, Wald A, Malhan C (The sink action of cerebrospinal fluid volume flow. Effect on brain water content. Arch Neurol 33:339-344.1976).

Hoffman EP, Fischbeck KH, Brown RH, Johnson M, Medori R, Loike JD, Harris JB, Waterston R, Brooke M, Specht L, . (Characterization of dystrophin in muscle-biopsy specimens from patients with Duchenne's or Becker's muscular dystrophy. N Engl J Med 318:1363-1368.1988).

Holm LM, Klaerke DA, Zeuthen T (Aquaporin 6 is permeable to glycerol and urea. Pflugers Arch 448:181-186.2004).

Ibraghimov-Beskrovnaya O, Ervasti JM, Leveille CJ, Slaughter CA, Sernett SW, Campbell KP (Primary structure of dystrophin-associated glycoproteins linking dystrophin to the extracellular matrix. Nature 355:696-702.1992).

Ishibashi K, Kuwahara M, Gu Y, Kageyama Y, Tohsaka A, Suzuki F, Marumo F, Sasaki S (Cloning and functional expression of a new water channel abundantly expressed in the testis permeable to water, glycerol, and urea. J Biol Chem 272:20782-20786.1997).

Ishibashi K, Morinaga T, Kuwahara M, Sasaki S, Imai M (Cloning and identification of a new member of water channel (AQP10) as an aquaglyceroporin. Biochim Biophys Acta 1576:335-340.2002).

Ishibashi K, Sasaki S, Fushimi K, Uchida S, Kuwahara M, Saito H, Furukawa T, Nakajima K, Yamaguchi Y, Gojobori T, . (Molecular cloning and expression of a member of the aquaporin family with permeability to glycerol and urea in addition to water expressed at the basolateral membrane of kidney collecting duct cells. Proc Natl Acad Sci U S A 91:6269-6273.1994).

Ito H, Yamamoto N, Arima H, Hirate H, Morishima T, Umenishi F, Tada T, Asai K, Katsuya H, Sobue K (Interleukin-1beta induces the expression of aquaporin-4 through a nuclear factor-kappaB pathway in rat astrocytes. J Neurochem 99:107-118.2006).

Itoh T, Rai T, Kuwahara M, Ko SB, Uchida S, Sasaki S, Ishibashi K (Identification of a novel aquaporin, AQP12, expressed in pancreatic acinar cells. Biochem Biophys Res Commun 330:832-838.2005).

Jaeger M, Soehle M, Meixensberger J (Effects of decompressive craniectomy on brain tissue oxygen in patients with intracranial hypertension. J Neurol Neurosurg Psychiatry 74:513-515.2003).

Joffe AR (Lumbar puncture and brain herniation in acute bacterial meningitis: a review. J Intensive Care Med 22:194-207.2007).

Johansson L, Rytkonen A, Wan H, Bergman P, Plant L, Agerberth B, Hokfelt T, Jonsson AB (Human-like immune responses in CD46 transgenic mice. J Immunol 175:433-440.2005).

Jung JS, Bhat RV, Preston GM, Guggino WB, Baraban JM, Agre P (Molecular characterization of an aquaporin cDNA from brain: candidate osmoreceptor and regulator of water balance. Proc Natl Acad Sci U S A 91:13052-13056.1994a).

Jung JS, Preston GM, Smith BL, Guggino WB, Agre P (Molecular structure of the water channel through aquaporin CHIP. The hourglass model. J Biol Chem 269:14648-14654.1994b).

Karwoski CJ, Lu HK, Newman EA (Spatial buffering of light-evoked potassium increases by retinal Muller (glial) cells. Science 244:578-580.1989).

Klatzo I (Pathophysiological aspects of brain edema. Acta Neuropathol 72:236-239.1987).

Koedel U, Klein M, Pfister HW (New understandings on the pathophysiology of bacterial meningitis. Curr Opin Infect Dis 23:217-223.2010).

Kofuji P, Ceelen P, Zahs KR, Surbeck LW, Lester HA, Newman EA (Genetic inactivation of an inwardly rectifying potassium channel (Kir4.1 subunit) in mice: phenotypic impact in retina. J Neurosci 20:5733-5740.2000).

Kornau HC, Schenker LT, Kennedy MB, Seeburg PH (Domain interaction between NMDA receptor subunits and the postsynaptic density protein PSD-95. Science 269:1737-1740.1995).

Kuriyama H, Kawamoto S, Ishida N, Ohno I, Mita S, Matsuzawa Y, Matsubara K, Okubo K (Molecular cloning and expression of a novel human aquaporin from adipose tissue with glycerol permeability. Biochem Biophys Res Commun 241:53-58.1997).

Kwon I, Kim EH, del Zoppo GJ, Heo JH (Ultrastructural and temporal changes of the microvascular basement membrane and astrocyte interface following focal cerebral ischemia. J Neurosci Res 87:668-676.2009).

Leclerc F, Walter-Nicolet E, Leteurtre S, Noizet O, Sadik A, Cremer R, Fourier C (Admission plasma vasopressin levels in children with meningococcal septic shock. Intensive Care Med 29:1339-1344.2003).

Lederfein D, Levy Z, Augier N, Mornet D, Morris G, Fuchs O, Yaffe D, Nudel U (A 71-kilodalton protein is a major product of the Duchenne muscular dystrophy gene in brain and other nonmuscle tissues. Proc Natl Acad Sci U S A 89:5346-5350.1992).

Lehmann A, Carlstrom C, Nagelhus EA, Ottersen OP (Elevation of taurine in hippocampal extracellular fluid and cerebrospinal fluid of acutely hypoosmotic rats: contribution by influx from blood? J Neurochem 56:690-697.1991).

Leib SL, Heimgartner C, Bifrare YD, Loeffler JM, Taauber MG (Dexamethasone aggravates hippocampal apoptosis and learning deficiency in pneumococcal meningitis in infant rats. Pediatr Res 54:353-357.2003).

Lin AL, Safdieh JE (The evaluation and management of bacterial meningitis: current practice and emerging developments. Neurologist 16:143-151.2010).

Liu JW, Wakayama Y, Inoue M, Shibuya S, Kojima H, Jimi T, Oniki H (Immunocytochemical studies of aquaporin 4 in the skeletal muscle of mdx mouse. J Neurol Sci 164:24-28.1999).

Lloyd-Jones D, Adams R, Carnethon M, De SG, Ferguson TB, Flegal K, Ford E, Furie K, Go A, Greenlund K, Haase N, Hailpern S, Ho M, Howard V, Kissela B, Kittner S, Lackland D, Lisabeth L, Marelli A, McDermott M, Meigs J, Mozaffarian D, Nichol G, O'Donnell C, Roger V, Rosamond W, Sacco R, Sorlie P, Stafford R, Steinberger J, Thom T, Wasserthiel-Smoller S, Wong N, Wylie-Rosett J, Hong Y (Heart disease and stroke statistics--2009 update: a report from the American Heart Association Statistics Committee and Stroke Statistics Subcommittee. Circulation 119:e21-181.2009).

Ma T, Yang B, Gillespie A, Carlson EJ, Epstein CJ, Verkman AS (Generation and phenotype of a transgenic knockout mouse lacking the mercurial-insensitive water channel aquaporin-4. J Clin Invest 100:957-962.1997).

Madrid R, Le MS, Barrault MB, Janvier K, Benichou S, Merot J (Polarized trafficking and surface expression of the AQP4 water channel are coordinated by serial and regulated interactions with different clathrin-adaptor complexes. EMBO J 20:7008-7021.2001).

Manley GT, Fujimura M, Ma T, Noshita N, Filiz F, Bollen AW, Chan P, Verkman AS (Aquaporin-4 deletion in mice reduces brain edema after acute water intoxication and ischemic stroke. Nat Med 6:159-163.2000).

McCoy ES, Haas BR, Sontheimer H (Water permeability through aquaporin-4 is regulated by protein kinase C and becomes rate-limiting for glioma invasion. Neuroscience 168:971-981.2010).

Melton JE, Patlak CS, Pettigrew KD, Cserr HF (Volume regulatory loss of Na, Cl, and K from rat brain during acute hyponatremia. Am J Physiol 252:F661-F669.1987).

Migliati E, Meurice N, DuBois P, Fang JS, Somasekharan S, Beckett E, Flynn G, Yool AJ (Inhibition of aquaporin-1 and aquaporin-4 water permeability by a derivative of the loop diuretic bumetanide acting at an internal pore-occluding binding site. Mol Pharmacol 76:105-112.2009).

Migliati ER, miry-Moghaddam M, Froehner SC, Adams ME, Ottersen OP, Bhardwaj A (Na(+)-K (+)-2Cl (-) Cotransport Inhibitor Attenuates Cerebral Edema Following Experimental Stroke via the Perivascular Pool of Aquaporin-4. Neurocrit Care.2010).

Milhorat TH (Classification of the cerebral edemas with reference to hydrocephalus and pseudotumor cerebri. Childs Nerv Syst 8:301-306.1992).

Moeller HB, Fenton RA, Zeuthen T, Macaulay N (Vasopressin-dependent short-term regulation of aquaporin 4 expressed in Xenopus oocytes. Neuroscience 164:1674-1684.2009).

Morishita Y, Matsuzaki T, Hara-Chikuma M, Andoo A, Shimono M, Matsuki A, Kobayashi K, Ikeda M, Yamamoto T, Verkman A, Kusano E, Ookawara S, Takata K, Sasaki S, Ishibashi K (Disruption of aquaporin-11 produces polycystic kidneys following vacuolization of the proximal tubule. Mol Cell Biol 25:7770-7779.2005).

Moritz ML, Ayus JC (Hospital-acquired hyponatremia--why are hypotonic parenteral fluids still being used? Nat Clin Pract Nephrol 3:374-382.2007).

Mulders SM, Preston GM, Deen PM, Guggino WB, van Os CH, Agre P (Water channel properties of major intrinsic protein of lens. J Biol Chem 270:9010-9016.1995).

Murata K, Mitsuoka K, Hirai T, Walz T, Agre P, Heymann JB, Engel A, Fujiyoshi Y (Structural determinants of water permeation through aquaporin-1. Nature 407:599-605.2000).

Nagelhus EA, Horio Y, Inanobe A, Fujita A, Haug FM, Nielsen S, Kurachi Y, Ottersen OP (Immunogold evidence suggests that coupling of K+ siphoning and water transport in rat retinal Muller cells is mediated by a coenrichment of Kir4.1 and AQP4 in specific membrane domains. Glia 26:47-54.1999).

Nassif X (Microbiology. A furtive pathogen revealed. Science 287:1767-1768.2000).

Neely JD, miry-Moghaddam M, Ottersen OP, Froehner SC, Agre P, Adams ME (Syntrophin-dependent expression and localization of Aquaporin-4 water channel protein. Proc Natl Acad Sci U S A 98:14108-14113.2001).

Nicchia GP, Rossi A, Nudel U, Svelto M, Frigeri A (Dystrophin-dependent and -independent AQP4 pools are expressed in the mouse brain. Glia 56:869-876.2008).

Nielsen S, Nagelhus EA, miry-Moghaddam M, Bourque C, Agre P, Ottersen OP (Specialized membrane domains for water transport in glial cells: high-resolution immunogold cytochemistry of aquaporin-4 in rat brain. J Neurosci 17:171-180.1997).

Niermann H, miry-Moghaddam M, Holthoff K, Witte OW, Ottersen OP (A novel role of vasopressin in the brain: modulation of activity-dependent water flux in the neocortex. J Neurosci 21:3045-3051.2001).

Orihuela CJ, Mahdavi J, Thornton J, Mann B, Wooldridge KG, Abouseada N, Oldfield NJ, Self T, a'Aldeen DA, Tuomanen EI (Laminin receptor initiates bacterial contact with the blood brain barrier in experimental meningitis models. J Clin Invest 119:1638-1646.2009).

Ostby I, Oyehaug L, Einevoll GT, Nagelhus EA, Plahte E, Zeuthen T, Lloyd CM, Ottersen OP, Omholt SW (Astrocytic mechanisms explaining neural-activity-induced shrinkage of extraneuronal space. PLoS Comput Biol 5:e1000272.2009).

Ottersen OP (Postembedding immunogold labelling of fixed glutamate: an electron microscopic analysis of the relationship between gold particle density and antigen concentration. J Chem Neuroanat 2:57-66.1989).

Papadopoulos MC, Manley GT, Krishna S, Verkman AS (Aquaporin-4 facilitates reabsorption of excess fluid in vasogenic brain edema. FASEB J 18:1291-1293.2004).

Papadopoulos MC, Verkman AS (Aquaporin-4 gene disruption in mice reduces brain swelling and mortality in pneumococcal meningitis. J Biol Chem 280:13906-13912.2005).

Papadopoulos MC, Verkman AS (Potential utility of aquaporin modulators for therapy of brain disorders. Prog Brain Res 170:589-601.2008).

Park JH, Saier MH, Jr. (Phylogenetic characterization of the MIP family of transmembrane channel proteins. J Membr Biol 153:171-180.1996).

Pedersen M, Brandt CT, Knudsen GM, Ostergaard C, Skinhoj P, Frimodt-Moller N, Moller K (Cerebral blood flow autoregulation in early experimental S. pneumoniae meningitis. J Appl Physiol 102:72-78.2007).

Preston GM, Agre P (Isolation of the cDNA for erythrocyte integral membrane protein of 28 kilodaltons: member of an ancient channel family. Proc Natl Acad Sci U S A 88:11110-11114.1991).

Preston GM, Jung JS, Guggino WB, Agre P (The mercury-sensitive residue at cysteine 189 in the CHIP28 water channel. J Biol Chem 268:17-20.1993).

Pujol C, Eugene E, Marceau M, Nassif X (The meningococcal PilT protein is required for induction of intimate attachment to epithelial cells following pilus-mediated adhesion. Proc Natl Acad Sci U S A 96:4017-4022.1999).

Pumain R, Heinemann U (Stimulus- and amino acid-induced calcium and potassium changes in rat neocortex. J Neurophysiol 53:1-16.1985).

Raina S, Preston GM, Guggino WB, Agre P (Molecular cloning and characterization of an aquaporin cDNA from salivary, lacrimal, and respiratory tissues. J Biol Chem 270:1908-1912.1995).

Rao JS, Steck PA, Mohanam S, Stetler-Stevenson WG, Liotta LA, Sawaya R (Elevated levels of M(r) 92,000 type IV collagenase in human brain tumors. Cancer Res 53:2208-2211.1993).

Rash JE, Yasumura T, Hudson CS, Agre P, Nielsen S (Direct immunogold labeling of aquaporin-4 in square arrays of astrocyte and ependymocyte plasma membranes in rat brain and spinal cord. Proc Natl Acad Sci U S A 95:11981-11986.1998).

Rojek A, Praetorius J, Frokiaer J, Nielsen S, Fenton RA (A current view of the mammalian aquaglyceroporins. Annu Rev Physiol 70:301-327.2008).

Rosenberg GA, Navratil M, Barone F, Feuerstein G (Proteolytic cascade enzymes increase in focal cerebral ischemia in rat. J Cereb Blood Flow Metab 16:360-366.1996).

Saadoun S, Papadopoulos MC, Davies DC, Krishna S, Bell BA (Aquaporin-4 expression is increased in oedematous human brain tumours. J Neurol Neurosurg Psychiatry 72:262-265.2002).

Saparov SM, Liu K, Agre P, Pohl P (Fast and selective ammonia transport by aquaporin-8. J Biol Chem 282:5296-5301.2007).

Schellinger PD, Kaste M, Hacke W (An update on thrombolytic therapy for acute stroke. Curr Opin Neurol 17:69-77.2004).

Silberstein C, Bouley R, Huang Y, Fang P, Pastor-Soler N, Brown D, Van Hoek AN (Membrane organization and function of M1 and M23 isoforms of aquaporin-4 in epithelial cells. Am J Physiol Renal Physiol 287:F501-F511.2004).

Simard JM, Kent TA, Chen M, Tarasov KV, Gerzanich V (Brain oedema in focal ischaemia: molecular pathophysiology and theoretical implications. Lancet Neurol 6:258-268.2007).

Sonnenblick M, Friedlander Y, Rosin AJ (Diuretic-induced severe hyponatremia. Review and analysis of 129 reported patients. Chest 103:601-606.1993).

Stephens DS, Greenwood B, Brandtzaeg P (Epidemic meningitis, meningococcaemia, and Neisseria meningitidis. Lancet 369:2196-2210.2007).

Sterns RH, Baer J, Ebersol S, Thomas D, Lohr JW, Kamm DE (Organic osmolytes in acute hyponatremia. Am J Physiol 264:F833-F836.1993).

Suzuki H, Nishikawa K, Hiroaki Y, Fujiyoshi Y (Formation of aquaporin-4 arrays is inhibited by palmitoylation of N-terminal cysteine residues. Biochim Biophys Acta 1778:1181-1189.2008).

Tagaya M, Haring HP, Stuiver I, Wagner S, Abumiya T, Lucero J, Lee P, Copeland BR, Seiffert D, del Zoppo GJ (Rapid loss of microvascular integrin expression during focal brain ischemia reflects neuron injury. J Cereb Blood Flow Metab 21:835-846.2001).

Thom M, Eriksson S, Martinian L, Caboclo LO, McEvoy AW, Duncan JS, Sisodiya SM (Temporal lobe sclerosis associated with hippocampal sclerosis in temporal lobe epilepsy: neuropathological features. J Neuropathol Exp Neurol 68:928-938.2009).

Thurston JH, Hauhart RE, Jones EM, Ater JL (Effects of salt and water loading on carbohydrate and energy metabolism and levels of selected amino acids in the brains of young mice. J Neurochem 24:953-957.1975).

Tonjum T (2005) Genus Neisseria. In Garrity G.M ed Bergey's Manual of System Bacteriology., pp 777-798: Springer Verlag New York, Inc.

Vajda Z, Promeneur D, Doczi T, Sulyok E, Frokiaer J, Ottersen OP, Nielsen S (Increased aquaporin-4 immunoreactivity in rat brain in response to systemic hyponatremia. Biochem Biophys Res Commun 270:495-503.2000).

van der WT, Tomassen SF, Houtsmuller AB, de Jonge HR, Tilly BC (Increased vesicle recycling in response to osmotic cell swelling. Cause and consequence of hypotonicity-provoked ATP release. J Biol Chem 278:40020-40025.2003).

Verbavatz JM, Ma T, Gobin R, Verkman AS (Absence of orthogonal arrays in kidney, brain and muscle from transgenic knockout mice lacking water channel aquaporin-4. J Cell Sci 110 (Pt 22):2855-2860.1997).

Walz T, Smith BL, Agre P, Engel A (The three-dimensional structure of human erythrocyte aquaporin CHIP. EMBO J 13:2985-2993.1994).

Warth A, Kroger S, Wolburg H (Redistribution of aquaporin-4 in human glioblastoma correlates with loss of agrin immunoreactivity from brain capillary basal laminae. Acta Neuropathol 107:311-318.2004).

Watson DA, Musher DM (Interruption of capsule production in Streptococcus pneumonia serotype 3 by insertion of transposon Tn916. Infect Immun 58:3135-3138.1990).

Weber JR, Tuomanen EI (Cellular damage in bacterial meningitis: an interplay of bacterial and host driven toxicity. J Neuroimmunol 184:45-52.2007).

Yasui M, Hazama A, Kwon TH, Nielsen S, Guggino WB, Agre P (Rapid gating and anion permeability of an intracellular aquaporin. Nature 402:184-187.1999a).

Yasui M, Kwon TH, Knepper MA, Nielsen S, Agre P (Aquaporin-6: An intracellular vesicle water channel protein in renal epithelia. Proc Natl Acad Sci U S A 96:5808-5813.1999b).

Zarantonelli ML, Szatanik M, Giorgini D, Hong E, Huerre M, Guillou F, Alonso JM, Taha MK (Transgenic mice expressing human transferrin as a model for meningococcal infection. Infect Immun 75:5609-5614.2007).

I

II

Temporary loss of perivascular aquaporin-4 in neocortex after transient middle cerebral artery occlusion in mice

Didrik S. Frydenlund*, Anish Bhardwaj[†‡], Takashi Otsuka[†], Maria N. Mylonakou*, Thomas Yasumura[§], Kimberly G. V. Davidson[§], Emil Zeynalov[†], Øivind Skare[¶], Petter Laake[¶], Finn-Mogens Haug*, John E. Rash[§‖], Peter Agre*[††], Ole P. Ottersen*[††], and Mahmood Amiry-Moghaddam*[††]

*Nordic Centre of Excellence for Research in Water Imbalance Related Disorders (WIRED), Centre for Molecular Biology and Neuroscience, Department of Anatomy, University of Oslo, P.O. Box 1105, 0317 Oslo, Norway; [¶]Department of Biostatistics, Institute for Basic Medical Sciences, University of Oslo, 0317 Oslo, Norway; Departments of [†]Anesthesiology and Critical Care Medicine and [‡]Neurology, Johns Hopkins University School of Medicine, Baltimore, MD 21205; [§]Department of Biomedical Sciences and [‖]Program in Molecular, Cellular, and Integrative Neuroscience, Colorado State University, Fort Collins, CO 80523-1617; and **Duke University School of Medicine, Durham, NC 27710

Contributed by Peter Agre, July 11, 2006

The aquaporin-4 (AQP4) pool in the perivascular astrocyte membranes has been shown to be critically involved in the formation and dissolution of brain edema. Cerebral edema is a major cause of morbidity and mortality in stroke. It is therefore essential to know whether the perivascular pool of AQP4 is up- or down-regulated after an ischemic insult, because such changes would determine the time course of edema formation. Here we demonstrate by quantitative immunogold cytochemistry that the ischemic striatum and neocortex show distinct patterns of AQP4 expression in the reperfusion phase after 90 min of middle cerebral artery occlusion. The striatal core displays a loss of perivascular AQP4 at 24 hr of reperfusion with no sign of subsequent recovery. The most affected part of the cortex also exhibits loss of perivascular AQP4. This loss is of magnitude similar to that of the striatal core, but it shows a partial recovery toward 72 hr of reperfusion. By freeze fracture we show that the loss of perivascular AQP4 is associated with the disappearance of the square lattices of particles that normally are distinct features of the perivascular astrocyte membrane. The cortical border zone differs from the central part of the ischemic lesion by showing no loss of perivascular AQP4 at 24 hr of reperfusion but rather a slight increase. These data indicate that the size of the AQP4 pool that controls the exchange of fluid between brain and blood during edema formation and dissolution is subject to large and region-specific changes in the reperfusion phase.

astrocytes | brain edema | ischemia | stroke | water channels

Stroke is invariably associated with a brain edema that accounts for much of the morbidity and mortality of this condition. The brain edema is often long lasting and therapy-resistant and thus poses a major challenge in the clinic. A better understanding is needed of the molecular mechanisms that promote water flux across the brain–blood interface in the build-up phase and resolution phase of cerebral edema.

Aquaporin-4 (AQP4) water channels are strongly enriched in the astrocyte plasma membrane domains that ensheathe the cerebral microvessels (1, 2). It was hypothesized (1) that this perivascular pool of AQP4 could become rate-limiting for water flux in pathophysiological conditions, such as in the reperfusion phase after an ischemic insult. This hypothesis was tested in a model that took advantage of the fact that the perivascular AQP4 pool is anchored through the dystrophin complex (comprising the brain dystrophin isoform DP-71 and α-syntrophin) (3). Mice with targeted deletion of α-syntrophin displayed a dramatic loss of perivascular AQP4 and a concomitant reduction in the extent of postischemic edema (4). These findings [and experiments in mdx mice (5)] support the idea that the perivascular pool of AQP4 facilitates water flux across the brain–blood interface and offer a mechanistic explanation for the reduction in brain edema formation and dissolution observed in AQP4$^{-/-}$ animals (6, 7) The implication of a specialized class of membrane molecule in the pathophysiology of brain edema instills hope for new therapy that could complement the current treatment strategies based on surgical decompression or infusion of hyperosmolar solutions.

A critical question is whether the perivascular pool of AQP4 is down- or up-regulated during or after a transient ischemic insult. If astrocytes respond to ischemia by down-sizing the perivascular pool of AQP4, this would delimit water uptake but would also reduce the potential for any therapeutic intervention targeting AQP4.

The aim of this work was to unravel the time course of AQP4 expression at the blood–brain interface, after transient ischemia induced by middle cerebral artery occlusion (MCAO). The postembedding immunogold procedure is uniquely suited to this task, because it offers a semiquantitative assessment of the AQP4 pool in distinct membrane domains (8). Immunoblot analyses are not relevant, because the total amount of AQP4 in the neuropil is poorly correlated with the size of the perivascular pool of this protein. Indeed, disruption of the anchoring of the endfoot pool of AQP4 led to a mislocalization, rather than a net loss of AQP4 (3).

Results

On the unaffected side (see *Materials and Methods*), double immunofluorescence analysis showed colocalization of AQP4 with dystrophin (Fig. 1*A*) and α-syntrophin (Fig. 1*C*) around brain microvessels. The same staining pattern was found in the border zone of the ischemic lesion and in ipsilateral cortical areas more distant from the lesion. In the central part of the ischemic neocortex, examined after 24 hr of reperfusion, the perivascular pools of dystrophin (Fig. 1*B*) and α-syntrophin (Fig. 1*D*) largely persisted, whereas the perivascular pool of AQP4 was lost. Only in deep regions of the cortex (and in the striatal core) were vessels found that lacked immunoreactivity for AQP4 as well as dystrophin and α-syntrophin.

Prompted by the results of the immunofluorescence analysis, we used a postembedding immunogold procedure to assess AQP4 expression in the perivascular astrocyte membrane (Figs. 2 and 3). The loss of perivascular AQP4 immunoreactivity in the

Conflict of interest statement: No conflicts declared.

Freely available online through the PNAS open access option.

Abbreviations: AQP4, aquaporin-4; MCAO, middle cerebral artery occlusion.

[††]To whom correspondence may be addressed. E-mail: mahmo@medisin.uio.no, o.p.ottersen@medisin.uio.no, or pagre@cellbio.duke.edu.

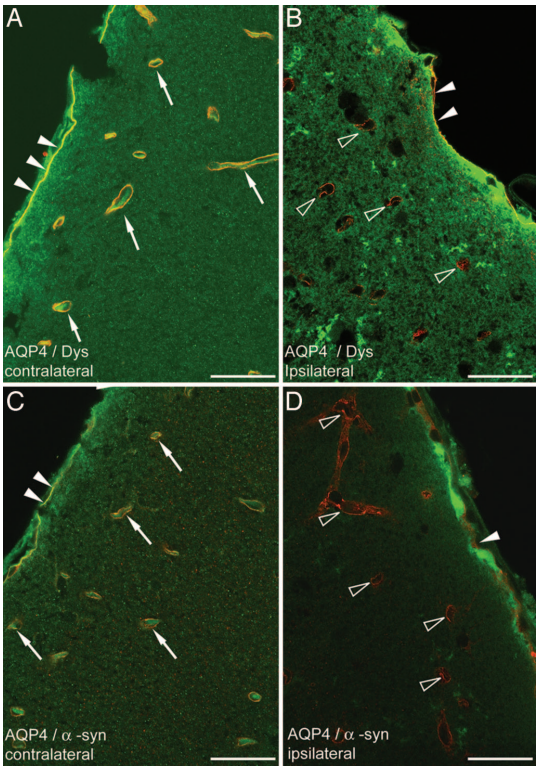

Fig. 1. Immunofluorescence analysis of brains subjected to MCAO (neocortex; 24 hr of reperfusion). (*A* and *C*) Contralateral neocortex, area opposite to ischemic core. (*B* and *D*) Central part of ischemic cortex (Fig. 5, region 4). Yellow labeling surrounding vessels in contralateral cortex indicates colocalization (arrows) of AQP4 (green) and dystrophin (red in *A*) and α-syntrophin (red in *C*). In contrast, vessels in the ischemic cortex are associated with a red signal (open arrowheads), indicating the absence of AQP4 and retention of dystrophin (*B*) and α-syntrophin (*D*). Filled arrowheads indicate the subpial endfeet. Dys, dystrophin; α-syn, α-syntrophin. (Scale bar: 20 μm.)

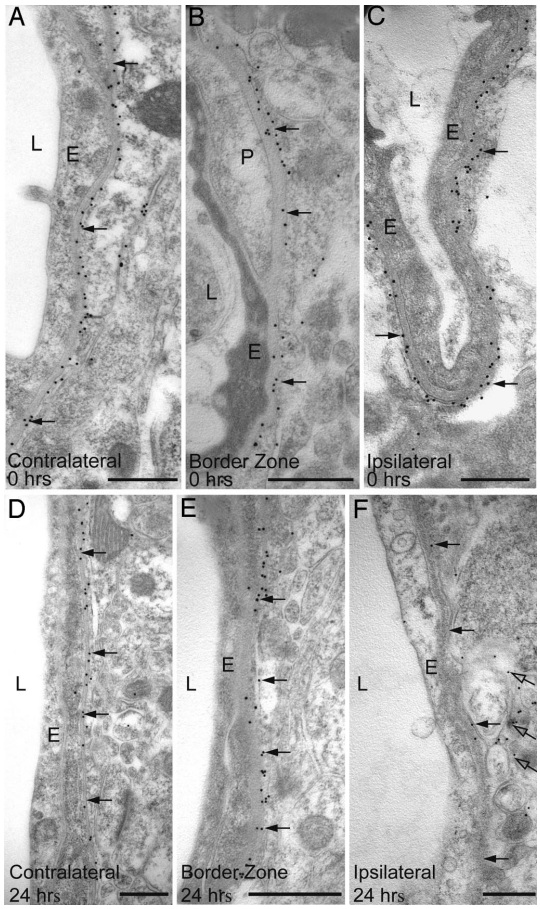

Fig. 2. Immunogold analysis of AQP4 expression immediately (0 hr in *A–C*) and 24 hr (*D–F*) after the onset of reperfusion (0 hr). At 24 hr, there is a pronounced reduction in the number of gold particles (arrows) over perivascular membranes in central part of the ischemic cortex (*F*) compared with the border zone (*E*) and contralateral side (*D*). In the ischemic cortex, AQP4 labeling remains over the abluminal membrane of the perivascular endfeet (open arrows in *F*). E, endothelial cells; L, vessel lumen; P, pericyte. (Scale bar: 0.5 μm.)

neocortical lesion at 24 hr of reperfusion was confirmed (Fig. 2*F*). Visual examination of earlier and later time points (including 0 hr, Fig. 2*C*) revealed no or more modest losses, suggesting that the perivascular AQP4 labeling reached minimum values at ≈24 hr.

The qualitative data were supplemented by a quantitative immunogold analysis of the striatal and neocortical zones of the ischemic lesion (Fig. 3). The contralateral side was used as an internal reference in each animal to minimize the confounding effect of possible differences in fixation efficiency. Each of the four animals analyzed at 24 hr of reperfusion showed a statistically significant loss of perivascular AQP4 in the central part of the ischemic cortex, compared with the corresponding part of the contralateral cortex (Fig. 3). On average, the labeling decreased by 78%, with a minimum of 59% and a maximum of 93%. In contrast, none of the animals displayed any significant loss of AQP4 from perivascular membranes of the cortical border zone. This was true for each group of animals, irrespective of reperfusion time. Indeed, the labeling in the border zone (the intensity of which was slightly depressed at the start of reperfusion) tended to increase toward 24 hr and thence to decrease toward control level (Fig. 3).

Supporting the qualitative analysis, the quantitative data suggested that the pronounced loss of perivascular AQP4 in the central part of the ischemic cortex at 24 hr was not a precipitous event but rather a trough preceded by a gradual decline and followed by a gradual restoration. Thus, at 24, 48, and 72 hr of reperfusion, the loss of AQP4 averaged 78%, 58%, and 45% with significance levels between 0.0058 and 0.0477. At 2 and 6 hr of reperfusion, the immunogold density values for AQP4 were 59% and 80% of control values, respectively, and were not significantly different from these values (*P* values of 0.07 and 0.36, respectively).

The data described above were obtained from the neocortex. We also investigated AQP4 expression in the striatum, which constitutes a major part of the ischemic core. The pattern of changes in the striatum mimicked the pattern of changes in the overlying neocortex, with one notable exception: The tendency

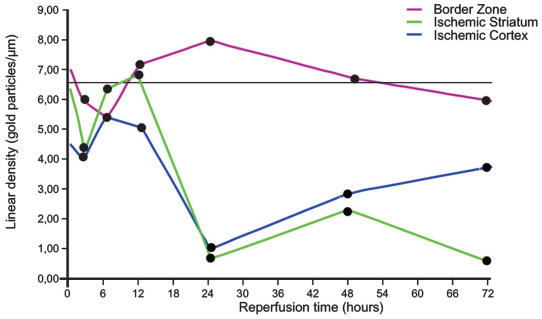

Fig. 3. Time course of AQP4 expression after MCAO. Values along the ordinate represent linear density of gold particles over perivascular membranes (same samples as in Fig. 2). Density values were obtained from the central part of the ischemic cortex (blue), striatal part of the core (green), and cortical border zone (red). The horizontal black line indicates the reference level (calculated from the neocortex and striatum contralateral to the lesion). The values for the ischemic cortex (blue) and striatal core (green) are significantly different from the reference values for reperfusion times of 24, 48, and 72 hr. The corresponding *P* values are 0.0058, 0.0122, and 0.0477 (cortex) and 0.0043, 0.0076, and 0.0052 (striatum), respectively.

toward a recovery of immunolabeling at 72 hr, obvious in the neocortex, was not observed in the striatum (Fig. 3).

In the central part of the ischemic cortex, the abluminal membrane of the endfeet showed scattered gold particles (Fig. 2*F*). This membrane domain is normally almost devoid of gold particles signaling AQP4. The quantitative immunogold analysis of the ischemic cortex revealed no alteration in the α-syntrophin expression level at 0 or 24 hr of reperfusion (data not shown).

Astrocyte endfeet were examined by freeze fracture (Fig. 4*A*). At high magnification, AQP4 square arrays were abundant in the endfoot membrane facing the capillary (Fig. 4*B*), and glial fibrillary acidic protein (GFAP) filaments were abundant in the cytoplasm (faintly detectable at the low magnification in Fig. 4*A*), with either marker providing for positive identification of astrocyte processes. In the border zone (Fig. 4 *C* and *D*), AQP4 square arrays were abundant in membrane P-faces abutting capillaries (Fig. 4*C*), and their imprints were abundant in endfoot membrane E-faces (Fig. 4*D*). The P-faces correspond to the replicated protoplasmic leaflet of split membranes, and the E-faces represent replicated extraplasmic membrane leaflets (9). Endfoot-like processes in the striatal core and overlying neocortex lacked AQP4 square arrays in their plasma membranes (Fig. 4*F*).

Discussion

The present work reveals that the expression level of the perivascular pool of AQP4 undergoes major changes after a transient ischemic insult. These results bear directly on the molecular mechanisms underlying the generation and dissolution of postischemic edema, because the perivascular pool of AQP4 allows bidirectional water flow and hence is likely to be rate-limiting for both water influx and efflux (4).

Our data suggest a biphasic change in perivascular AQP4 expression in the most affected part of the ipsilateral cortex. The initial reduction in AQP4 expression (with minimum values at $\approx$24 hr) will serve to delimit water influx, whereas the partial recovery of the AQP4 level (from 24 to 72 hr; i.e., subsequent to the culmination of the edema) would be expected to favor absorption of excess fluid. This pattern of changes contrasts with the changes that occur in the cortical border zone. Here, a trend toward an elevated level of AQP4 expression was observed at a

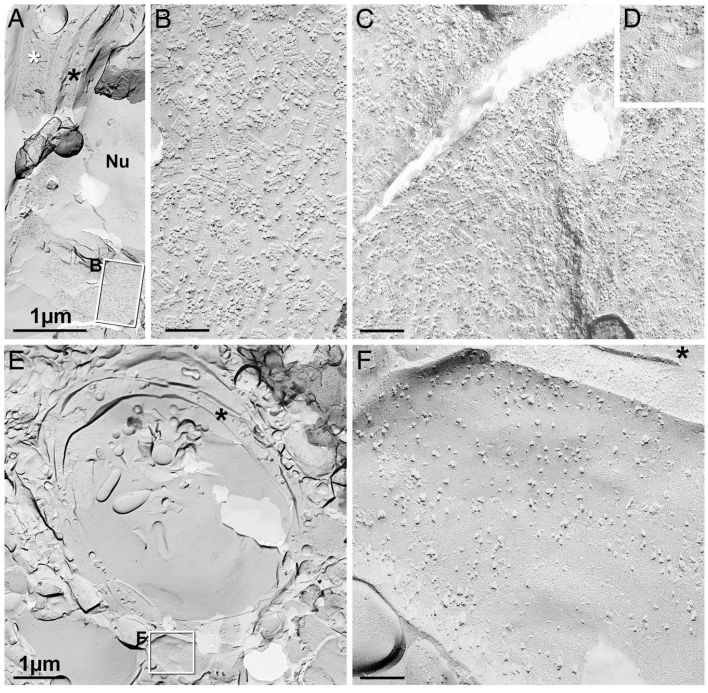

Fig. 4. Conventional freeze fracture images from contralateral cortex (*A* and *B*), cortical border zone (*C* and *D*), and central part of ischemic lesion (*E* and *F*), all from 24 hr of reperfusion after MCAO. (*A*) Low-magnification image from contact region between astrocyte endfoot (white asterisk) and the edge of capillary (black asterisk in cytoplasm). Boxed area encloses P-face of astrocyte, shown at higher magnification in *B*. Nu, endothelial nucleus. (*B*) High-magnification view of P-face of astrocyte endfoot plasma membrane, showing >100 AQP4 arrays in $\approx$0.3 μm^2. (*C*) P-face of astrocyte endfoot in border zone has AQP4 arrays at approximately the same density as in contralateral control. (*D*) E-face view of AQP4 imprints, also from border zone. (*E*) Low-magnification view of capillary in central part of ischemic lesion. Membrane debris is present in the lumen of the capillary. Boxed area including presumptive astrocyte endfoot shown at higher magnification in *F*. The black asterisk indicates endothelial cytoplasm. (*F*) High-magnification image of E-face of presumptive astrocyte endfoot in central part of ischemic lesion. AQP4 arrays were not detected in this or any other membrane adjacent to capillaries. The black asterisk indicates endothelial cytoplasm. *B*–*D* and *F* are at the same magnification. (Calibration bars: *A* and *E*, 1 μm; *B*, *C*, and *F*, 0.1 μm.)

time when the AQP4 expression was decreased in the central part of the ischemic cortex.

The present data clearly show that the cortical region most severely affected by the ischemic insult behaves differently from the striatal core when it comes to changes in AQP4 expression in the postischemic phase. Notably, unlike the striatal core, the ischemic cortex shows a partial recovery of perivascular AQP4 toward 72 hr of reperfusion. Taken together with our finding of persistent α-syntrophin and dystrophin labeling, the latter observation suggests that the affected cortex (with the possible exception of the deepest layers) differs from the striatal core by preserving, for 72 hr at least, the integrity of astrocyte membranes after the MCAO insult. On this background we have chosen to distinguish the affected cortex from the striatal core by using the term "central part of the ischemic cortex" rather than the term "cortical core."

The persistence in the cortex of dystrophin and α-syntrophin in the perivascular membrane leaves us with a mechanistic model in which ischemia disrupts the coupling between AQP4 and its anchoring complex. Rapid changes in the size of the perivascular AQP4 pool can be envisaged if the anchoring is severed, because of the high AQP4 concentration gradient between perivascular membranes and other membrane domains (including the abluminal endfoot membrane, which showed increased labeling after ischemia). Our findings are consistent with the idea that an ischemia-induced perturbation of AQP4 anchoring permits a lateral diffusion of AQP4, thereby draining the pool of AQP4 that normally resides in the perivascular membrane. This explanation is in line with previous observations in transfected HEK 293 cells, indicating that truncated AQP4 (lacking the three C-terminal residues that are essential for binding to the dystrophin complex) disappears much more quickly from the membranes than WT AQP4 (3).

Theoretically, the loss of AQP4 immunosignal could be due to conformational changes in AQP4 with a subsequent loss of affinity for the selective antibodies. This possibility could be ruled out by the freeze fracture analysis, which demonstrated a complete loss of the square lattices of particles from the endfoot membranes. Expression studies and analysis of AQP4-null animals have provided conclusive evidence that these square lattices correspond to arrays of AQP4 (10, 11).

We have previously shown by Western blotting that disruption of AQP4 anchoring at the perivascular membrane leads to a mislocalization of AQP4 rather than a net loss (3, 8). Previous studies of the effects of ischemia on AQP4 have not focused on the perivascular (rate-limiting) pool of AQP4 but have analyzed the tissue contents of AQP4 or the level of AQP4 mRNA (12–14). There is evidence of an increased synthesis of AQP4 in the periinfarct zone after MCAO or stroke (14).

The persistence of the perivascular AQP4 pool in the cortical border zone suggests that partial ischemia is not sufficient to interfere significantly with anchoring of AQP4 (although the initial drop in AQP4 expression may be indicative of a transient effect on the anchoring mechanisms). This finding could be exploited diagnostically in attempts to assess the relative volumes of the central part and border zone of the ischemic lesion, given the availability of a ligand that binds selectively to the perivascular pool of AQP4. Our findings are in agreement with a recent study (15) which shows that osmotherapy with 7.5% hyperosmotic saline at 24 hr after MCAO in rats leads to a significant decrease in the brain water content in the cortical border zone (where the perivascular AQP4 expression is retained) but not in the central part of the lesion (where the perivascular AQP4 expression is strongly reduced).

In conclusion, our data suggest that the size of the AQP4 pool that controls the exchange of fluid between brain and blood during edema formation and dissolution is subject to large changes during the reperfusion phase. The magnitude and direction of these changes serve to distinguish the central part from the border zone of the ischemic lesion and must be taken into account in future strategies to develop new therapies targeting AQP4 or associated molecules in the perivascular membrane.

Materials and Methods

Animals. Experimental protocols were approved by the Institutional Animal Care and Use Committee and conform to National Institute of Health guidelines for the care and use of animals. Studies were conducted with male WT C57BL mice allowed ad libitum access to food and drinking water.

Brain Ischemia. Twenty-one mice with body weights of 27–32 g were anesthetized with 1–1.2% halothane in oxygen-enriched air, and rectal temperature was maintained at 37 $\pm$ 0.5°C with heating lamps during the entire surgical procedure. Mice were then subjected to MCAO in a randomized fashion as described previously (4). MCAO was verified at 30 min by allowing the animal to awaken and performing neurological deficit scoring as follows: 0, normal motor function; 1, flexion of torso and of contralateral forelimb upon lifting by the tail; 2, circling to the contralateral side but normal posture at rest; 3, leaning to the contralateral side at rest; 4, no spontaneous motor activity. Mice with clear neurological deficits (score of $\geq$2) were reanesthetized for withdrawal of the suture and reperfusion after 90 min of MCAO. The mice were perfused for immunocytochemistry at different time points after the onset of reperfusion (0, 2, 6, 12, 24, 48, and 72 hr). A few animals were excluded because of subarachnoidal hemorrhage. The final numbers of animals included for electron microscopic analysis were three for 0, 2, 6, 12, and 48 hr of reperfusion; four for 24 hr of reperfusion; and two for 72 hr of reperfusion. Two additional animals were perfused at 24 hr for immunofluorescence analysis. The use of the contralateral side as reference gave statistical significance with a relatively low number of animals (see below).

Tissue was sampled from the striatal core and the overlying neocortex (the "central part of the ischemic cortex"). Samples were also collected from the neocortical border zone (defined as the most peripheral zone of the affected cortex and with less distinct pallor than the core).

Antibodies. Antibodies to AQP4 (polyclonal, Alpha Diagnostics, San Antonio, TX; monoclonal, Serotec, Oxford, U.K.), α-syntrophin [polyclonal (16)], or dystrophin (polyclonal, raised against the C terminus of DP-71; Abcam, Cambridge, U.K.) were used in the present work. The properties of the antibodies have been described (3, 17, 18). The selectivity of the labeling was confirmed by omission of the primary antibody or preadsorption with the immunizing peptide.

Electron Microscopy. Mice were perfused through the heart with 4% formaldehyde in phosphate buffer at pH 6.0, then pH 10.0 (4). For quantitative immunogold studies, tissue blocks were dissected from a 1.0-mm-thick coronal slice through the forebrain. The tissue blocks did not exceed 1 mm in any dimension and were dissected from each of the following five regions (Fig. 5): 1, contralateral neocortex; 2, contralateral striatum; 3, cortical border zone; 4, central part of the ischemic cortex; and 5, striatal core. The tissue blocks were cryoprotected, quick-frozen in liquid propane (−170°C), and subjected to freeze substitution (3, 19). Specimens were embedded in methacrylate resin (Lowicryl HM20; Polysciences, Warrington, PA) and polymerized by UV light below 0°C. Ultrathin sections were incubated with antibodies to AQP4 (polyclonal, 10 μg/ml) or α-syntrophin (1:100) followed by goat anti-rabbit antibody coupled to 15-nm colloidal gold. The sections were examined in a Philips (Eindhoven, The Netherlands) CM10 electron microscope at 60 kV (20, 21).

Fluorescence Microscopy. For immunofluorescence we used 16-μm cryostat sections obtained from brains that had been fixed

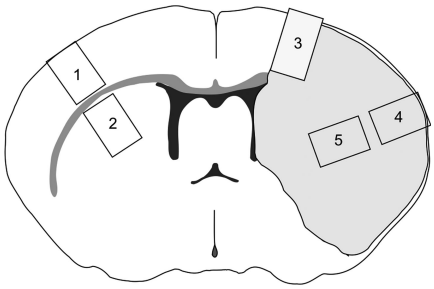

Fig. 5. Diagram of coronal slice through the forebrain. The shaded area on the right side is the area affected by ischemia. Specimens were dissected from the following: 1, contralateral neocortex (control); 2, contralateral striatum (control); 3, cortical border zone; 4, central part of ischemic cortex; and 5, striatal part of the ischemic core.

as described above. The sections were incubated with an antibody to AQP4 (monoclonal, 10 μg/ml) together with anti-dystrophin (5 μg/ml) or anti-syntrophin (1:500) followed by Alexa Fluor 448-conjugated donkey anti-mouse and Cy3-conjugated goat anti-rabbit IgG antibodies and were then viewed and photographed with a Zeiss (Oberkochen, Germany) LSM 5 Pascal confocal microscope (8).

Freeze Fracture. Formaldehyde-fixed tissue blocks from the core region, the border zone, and the contralateral cortex were sectioned at 150 μm, infiltrated with 30% glycerol, frozen by contact with a liquid nitrogen-cooled metal mirror (ULTRA-FREEZE MF7000; RMC Products, Tucson, AZ), fractured and replicated in an RMC/JEOL (JEOL, Tokyo, Japan) 9010c freeze fracture machine, and cleaned with 5.25% sodium hypochlorite bleach (22). Replicas were examined at 100 kV in a JEOL (Peabody, MA) 2000 EX-II transmission electron microscope (TEM). Astrocyte endfeet adjacent to capillaries were photographed stereoscopically at magnifications of $\times$10,000–50,000, with 8° included angle between images. TEM negatives were scanned and digitized by using an ArtixScan 2500f digital scanner (Microtek, Carson, CA) and processed with Adobe Photoshop CS by using minimal (or no) "unsharp mask," maximal contrast expansion with "levels," and selected area "dodging" using brightness/contrast functions to optimize image contrast and definition.

Quantification and Statistical Analysis. For the quantification of AQP4 immunogold labeling, 15–20 digital (16-bit) images from each section (one section per block, giving a total of 1,426 images) were acquired in a blinded manner and quantified with a commercially available image analysis program (analySIS; Soft Imaging Systems, Münster, Germany) (8, 17). Perivascular labeling was measured as gold particles per unit length of astrocyte membrane in direct contact with the pericapillary basal lamina (linear particle density). Particles were included if their centers were localized within 30 nm of the midpoint of the membrane (23). Linear densities of gold particles over astrocyte membranes were determined by an extension of analySIS (Soft Imaging Systems) as described (8, 24). Curves were drawn interactively, and linear densities were determined semiautomatically and transferred to SPSS Version 13 (SPSS, Chicago, IL). Values for individual curve segments were averaged per section (block, animal).

Data were analyzed by a linear mixed model, using the lme function in R (25). Fixed effects were first included for every combination of region and reperfusion time. We assumed a dependency structure with random effects on animals and on regions inside animals. Parameter estimates were obtained by maximum likelihood for the fixed effects and by restricted maximum likelihood for the variances of the random effects. It was found that there were no significant difference in gold particle densities over times for the control regions (contralateral neocortex and striatum; P value of 0.434). Hence, we chose to represent these two regions by a single fixed effect. We assumed a model with variances that differ between regions. For a detailed description see www.med.uio.no/imb/stat/immunogold/index.html.

This work was supported in part by U.S. Public Health Service National Institutes of Health Grant NS 046379 (to A.B.), National Institutes of Health Grants NS 44395 and NS 44010 (to J.E.R.), the Norwegian Research Council, and NordForsk (Nordic Centre of Excellence Program in Molecular Medicine).

1. Nielsen, S., Nagelhus, E. A., Amiry-Moghaddam, M., Bourque, C., Agre, P. & Ottersen, O. P. (1997) *J. Neurosci.* **17,** 171–180.
2. Rash, J. E., Yasumura, T., Hudson, C. S., Agre, P. & Nielsen, S. (1998) *Proc. Natl. Acad. Sci. USA* **95,** 11981–11986.
3. Neely, J. D., Amiry-Moghaddam, M., Ottersen, O. P., Froehner, S. C., Agre, P. & Adams, M. E. (2001) *Proc. Natl. Acad. Sci. USA* **98,** 14108–14113.
4. Amiry-Moghaddam, M., Otsuka, T., Hurn, P. D., Traystman, R. J., Haug, F. M., Froehner, S. C., Adams, M. E., Neely, J. D., Agre, P., Ottersen, O. P., *et al.* (2003) *Proc. Natl. Acad. Sci. USA* **100,** 2106–2111.
5. Vajda, Z., Pedersen, M., Fuchtbauer, E. M., Wertz, K., Stodkilde-Jorgensen, H., Sulyok, E., Doczi, T., Neely, J. D., Agre, P., Frokiaer, J., *et al.* (2002) *Proc. Natl. Acad. Sci. USA* **99,** 13131–13136.
6. Manley, G. T., Fujimura, M., Ma, T., Noshita, N., Filiz, F., Bollen, A. W., Chan, P. & Verkman, A. S. (2000) *Nat. Med.* **6,** 159–163.
7. Papadopoulos, M. C., Manley, G. T., Krishna, S. & Verkman, A. S. (2004) *FASEB J.* **18,** 1291–1293.
8. Amiry-Moghaddam, M., Xue, R., Haug, F. M., Neely, J. D., Bhardwaj, A., Agre, P., Adams, M. E., Froehner, S. C., Mori, S. & Ottersen, O. P. (2004) *FASEB J.* **18,** 542–544.
9. Branton, D., Bullivant, S., Gilula, N. B., Karnovsky, M. J., Moor, H., Muhlethaler, K., Northcote, D. H., Packer, L., Satir, B., Satir, P., *et al.* (1975) *Science* **190,** 54–56.
10. Furman, C. S., Gorelick-Feldman, D. A., Davidson, K. G., Yasumura, T., Neely, J. D., Agre, P. & Rash, J. E. (2003) *Proc. Natl. Acad. Sci. USA* **100,** 13609–13614.
11. Verbavatz, J. M., Ma, T., Gobin, R. & Verkman, A. S. (1997) *J. Cell Sci.* **110,** 2855–2860.
12. Lu, H. & Sun, S. Q. (2003) *Chin. Med. J. (Engl. Ed.)* **116,** 1063–1069.
13. Meng, S., Qiao, M., Lin, L., Del Bigio, M. R., Tomanek, B. & Tuor, U. I. (2004) *Eur. J. Neurosci.* **19,** 2261–2269.
14. Taniguchi, M., Yamashita, T., Kumura, E., Tamatani, M., Kobayashi, A., Yokawa, T., Maruno, M., Kato, A., Ohnishi, T., Kohmura, E., *et al.* (2000) *Brain Res. Mol. Brain Res.* **78,** 131–137.
15. Chen, C. H., Toung, T. J., Sapirstein, A. & Bhardwaj, A. (2006) *J. Cereb. Blood Flow Metab.* **26,** 951–958.
16. Peters, M. F., Adams, M. E. & Froehner, S. C. (1997) *J. Cell Biol.* **138,** 81–93.
17. Amiry-Moghaddam, M., Williamson, A., Palomba, M., Eid, T., de Lanerolle, N. C., Nagelhus, E. A., Adams, M. E., Froehner, S. C., Agre, P. & Ottersen, O. P. (2003) *Proc. Natl. Acad. Sci. USA* **100,** 13615–13620.
18. Amiry-Moghaddam, M., Frydenlund, D. S. & Ottersen, O. P. (2004) *Neuroscience* **129,** 999–1010.
19. Takumi, Y., Ramirez-Leon, V., Laake, P., Rinvik, E. & Ottersen, O. P. (1999) *Nat. Neurosci.* **2,** 618–624.
20. Amiry-Moghaddam, M., Lindland, H., Zelenin, S., Roberg, B. A., Gundersen, B. B., Petersen, P., Rinvik, E., Torgner, I. A. & Ottersen, O. P. (2005) *FASEB J.* **19,** 1459–1467.
21. Puwarawuttipanit, W., Bragg, A. D., Frydenlund, D. S., Mylonakou, M. N., Nagelhus, E. A., Peters, M. F., Kotchabhakdi, N., Adams, M. E., Froehner, S. C., Haug, F. M., *et al.* (2006) *Neuroscience* **137,** 165–175.
22. Rash, J. E. & Yasumura, T. (1992) *Microsc. Res. Tech.* **20,** 187–204.
23. Matsubara, A., Laake, J. H., Davanger, S., Usami, S. & Ottersen, O. P. (1996) *J. Neurosci.* **16,** 4457–4467.
24. Mathiisen, T. M., Nagelhus, E. A., Jouleh, B., Torp, R., Frydenlund, D. S., Mylonakou, M.-N., Amiry-Moghaddam, M., Covolan, L., Utvik, J. K., Riber, B., *et al.* (2006) in *Neuroanatomical Tract-Tracing 3: Molecules, Neurons, and Systems*, eds. Zaborszky, L., Wouterlood, F. G. & Lanciego, J. L. (Springer, New York), pp. 72–108.
25. Pinheiro, J. C. & Bates, D. M. (2002) *Mixed Effects Models in S and S-PLUS* (Springer, New York).

III

IV